sciendo

Bulletin of Geography. Physical Geography Series, No. 19 (2020): 43–69
http://dx.doi.org/10.2478/bgeo-2020-0009

Analysing flood history and simulating the nature of future floods using Gumbel method and Log-Pearson Type III: the case of the Mayurakshi River Basin, India

ISSN 2080-7686

OPEN ACCESS

Aznarul Islam, Biplab Sarkar

Aliah University, Kolkata, West Bengal, India

Correspondence: Aliah University, Kolkata, West Bengal, India. E-mail: aznarulislam@gmail.com

https://orcid.org/0000-0003-2380-3909

Abstract. Floods of the Mayurakshi River Basin (MRB) have been historically documented since 1860. The high magnitude, low-frequency flood events have drastically changed to low magnitude, high-frequency flood events in the post-dam period, especially after the 1950s, when the major civil structures (Massanjore dam, Tilpara barrage, Brahmani barrage, Deucha barrage, and Bakreshwar weir) were constructed in the MRB. The present study intends to find out the nature of flood frequency using the extreme value method of Gumbel and Log-Pearson type III (LP-III). The results show that the highest flood magnitude (11,327 $m^3 s^{-1}$) was observed during 1957–2009 for the Tilpara barrage with a return probability of 1.85% and the lowest (708 $m^3 s^{-1}$) recorded by the Bakreshwar weir during 1956–77 with a return probability of 4.55%. In the present endeavour, we have computed the predicted discharge for the different return periods, like 2, 5, 10, 25, 50,100, and 200 years. The quantile-quantile plot shows that the expected discharge calculated using LP-III is more normally distributed than that of Gumbel. Moreover, Kolmogorov–Smirnov (KS) test, Anderson–Darling (AD), and x2 distribution show that LP-III distribution is more normally distributed than the Gumbel at 0.01 significance level, implying its greater reliability and acceptance in the flood simulation of the MRB.

Key words:
flood forecasting,
flood frequency analysis,
flood probability,
goodness of fit,
return period

Introduction

Flood is a common hazard found in the low-lying areas of the floodplains, deltas and coastal areas of the world. Globally flood has taken a toll of 6.8 million deaths in the 20th century (Doocy et al. 2013). In Asia flood was the largest disaster to plague nations like Bangladesh, India, and China in 2015 (Guha-Sapir et al. 2016). Flood frequently disrupts normal life by inducing direct consequences such as damage to buildings and infrastructure and indirect consequences such as public services breaking down outside the flooded territory. Similarly, floods have intangible effects on the psyche of the people and cause trauma (Nicholls et al. 2015). Generally, there are two recognised strategies – structural, or "hard" (e.g. dams and barrages), and non-structural or "soft" (e.g. land-use planning or flood forecasting) (Kundzewicz et al. 2019). In recent decades, with the increase in environmental consciousness "soft" measures are becoming more popular. Thus, flood frequency analysis (FFA) and flood forecasting have become a dominant trend of investigation in flood geomorphology. The probability of the FFA relies on long-term hydrological data (30 years or more) without breaks (Holmes 2014). Thus, small size of data, or lack of continuity in data, often result in an improbable FFA (Bobee et al. 1993; Hosking and Wallis 2005). Previous researchers (e.g. Pilon and Adamowski 1993; Cohn et al. 1997; Wal-

ters 2002; Reis et al. 2005) have developed realistic flood prediction models based on the FFA. Lázaro et al. (2016) found that Log-Pearson and Water Resources Council (WRC) methods are the most reliable methods, as compared to methods including Gumbel, Normal, Lognormal, Chow or Log-Pearson type III for the Spanish catchments. However, in the Indian context, due to the climatic variability of the Indian Monsoon, Gumbel and log-Pearson type III distributions are more commonly applied to study the extremities in rainfall and flood. For example, Kumar et al. (2014) applied the extreme value theory of Gumbel to rainfall patterns to conclude that rainfall increases with return periods. Additionally, Guru and Jha (2015) carried out an FFA of the Mahanadi system using generalised Pareto (GP), Lognormal distribution where annual maxima were better fitted on GP, while peak over the threshold (POT) better fitted to Lognormal. Moreover, Bhat et al. (2019) found Log-Pearson III to be more reliable compared to the Gumbel method while analysing the flood frequency of the Jhelam River in Kashmir, India. Similarly, Kumar (2019) also observed Log-Pearson III to be more appropriate than Gumbel extreme value 1 method while simulating the floods of the Rapti River, a tributary of the Ghaghra rivers system, India.

The floods of the Lower Ganga Plains (LGB) are fascinating and deserve special attention because flood hazard is the highest-rated hazard in this region for wide-encompassing and devastating nature that wreaks havoc on society almost every year (Islam et al. 2012). The floods of this region are diversified in terms of trigger mechanisms such as flash floods, riverine floods, and coastal floods including storm surges. Karmokar and De (2020) attempted flash flood risk assessment of the Himalayan foothill regions in West Bengal using a holistic outlook including the geology, morphometry, soil, climate and LULC characteristics of the basins. They found that the railway line and highways in the piedmont region of Jalpaiguri and Darjeeling Districts are the most susceptible areas. Similarly, Ghosh and Ghosal (2020) outlined the catastrophic nature of flash floods in the Himalayan foothills due to climate change.

However, the majority of discourse related to LGP floods is concerned with the nature, impact and management of fluvial floods because of their widespread nature. For example, Kapuria and Modak (2019) outlined monsoon-related high flows in the Ganga-Padma system to review the existing flood management strategies and prepare comprehensive and sustainable flood management strategies including structural and non-structural measures based on the integration of environmental, ecological, social, economic, climatological and institutional perspectives. Moreover, Rudra (2020) examined human interventions – especially the Farakka Barrage Project – to interrupt the environmental flow in the lower Ganga River. The study also found that frequent disturbance fluvial, marine and coastal processes lead to devastating floods in this fragile region. The work emphasises the integration of institutional and ecological issues for constructive and sustainable flood abatement strategies instead of mere structural interventions. Similarly, Mazumder (2004) examined the combined role that rising high flood levels of the Farakka Barrage, deposition of sediment upstream of the barrage and unprecedented rainfall in the Ganga-Mahananda interfluve all had on the disastrous flood of Malda in 1998. Moreover, Mollah and Bandapadhyay (2014) studied flood risk in the Murshidabad district in the context of population-development and environmental nexus. Using factor analysis, they proved that spatial variability of the vulnerability is based on community characteristics. Similarly, Mollah (2016) applied RIDIT analysis to demonstrate that the perception of the flood victims varies as per the geographic locations of the hamlets in the Murshidabad district. Besides, Bhattacharjee and Behere (2018) constructed a composite vulnerability index based on the functions of exposure, sensitivity and adaptive capacity at the household level. The study found that age of the household head, household income, landholding size and family size determine the adaptive capacity of the local people, while coping strategies are determined by: borrowing money from friends, relatives and moneylenders; selling assets and livestock; diversification of livelihoods; migration; the elevation of houses; and food and fuel stocks.

Furthermore, the floods of the western tributaries to the Bhagirathi-Hooghly River such as Damodar and Ajay are well explored. For example, Bhattacharyya (2011) examined the nature of floods due to the altered hydrologic regime of the

 Citation: Bulletin of Geography. Physical Geography Series 2020, 19, http://dx.doi.org/10.2478/bgeo-2020-0009

Damodar Valley Corporation (DVC). This study has depicted the adjustment mechanism of the self-settled refugees to live with floods. Similarly, Roy et al. (2020) applied support vector machine (SVM), random forest (RF), and biogeography based optimisation (BBO) in geographic information system (GIS) to detect the flood susceptibility of the Ajay River Basin, and concluded that the BBO shows the best-fit results in the monsoon dominated regions. Besides this, Das et al. (2019) studied the devastating nature of floods of Arambag area located in the interfluvial zones of the Damodar-Dwarakeswar River. They identified optimal location and the flood shelter based on analytical hierarchic process (AHP) and GIS-coupled field investigations for the mitigation of flood hazards.

Furthermore, coastal floods of the Medinipur coastal plain and Sundarban area are also noted. For example, Kaur et al. (2017) applied predictive modelling and overlay analysis to find out the spatial association between geo-environmental factors and floods of the Medinipur coastal plains. The geo-spatial modelling indicates that East Medinipur is more susceptible to floods than West Medinipur. Similarly, Sahana and Sajjad (2019) assessed the village -level vulnerability due to storm surge floods in the Sundarban Biosphere Reserve (SBR) based on the function of exposure, sensitivity and resilience. The study proposed a composite vulnerability model considering these three functions, which point out that the villages in the southern part of the Sundarban have higher vulnerability compared to the central part. Additionally, Sahana et al. (2020) attempted a flood susceptibility assessment of the SBR using frequency ratio, modified frequency ratio and SVM, and found that the SVM is the best-fit model for analysing susceptibility to storm-surge-related floods in the SBR.

The historical record indicates the severity of flood in the Mayurakshi River Basin (MRB). The nature and extent of flood in this area is well documented in some works, notably of Chaudhury (1966), Chakrabarti (1985), Jha and Bairagya (2012), Mukhopadhyay and Let (2014), the *Flood Preparedness and Management Plan* of the Office of the District Magistrate (2014; 2016) and Mollah (2016). Virtually all these works have a specific focus on the genesis of the flood, types of flood, number of flood victims, and extent of flood. However, Ghosh and Mukhopadhyay (2015) showed that the nature of the historic flood of the Tilpara barrage over the Mayurakshi River using Log-Pearson III and showed that flood frequency has increased in the post-dam period. Similarly, Ghosh and Pal (2015) also noted that FFA for the Massanjore and Tilpara over the Mayurakshi was more reliably computed using the Log-Pearson III than using the Gumbel extreme value method. Thus, it is observed that the FFA is done only for the Mayurakshi River, a part of the MRB. However, analysing flood frequency and simulating the future floods over the other sub-systems of the MRB such as the Dwarka, Brahmani, and Kuea is not attempted as far as the previously available literature is concerned. Therefore, this study will outline a comparative FFA taking the considerations of the major systems of the MRB that will help the researchers and regional planners to understand how the mechanisms of floods vary as per the variation of the hydro-geomorphic and anthropogenic attributes in different areas. Thus, the present inquiry attempts to address the following objectives.

- To find out the nature of flood frequency and predicted flood discharge using the extreme value method of Gumbel and Log-Pearson III methods,
- To assess the goodness of fit of the methods used in this study
- To examine the major drivers of the flood in the basin.

Study area

Mayurakshi River Basin (MRB) extends from 23˚37′43″N to 24˚37′36″N latitude and 86˚ 50′16″E to 88˚15′52″E longitude covering an area of about 9,596 km^2 in the states of Jharkhand and West Bengal (Fig. 1). The western part of the basin, located mainly in the Dumka district of Jharkhand, is a part of the Chhotonagpur Plateau, while the eastern part of the basin, located in the Birbhum and Murshidabad districts of West Bengal, is a part of the Ganga plains. And between the plateau and plain is a plateau fringe located in Birbhum district. Therefore, the MRB is located in such an area that it bears a long geological history with promi-

nent tectonic controls. There are traces of evidence of at least three erosion surfaces implying the activeness of the tectonic movements (Chakrabarti 1970). However, in the Anthropocene, control over the MRB is strongly observed through the structural controls induced by dams and barrages. There are five major civil structures, these being Massanjore dam and Tilpara barrage on the Mayurakshi River,

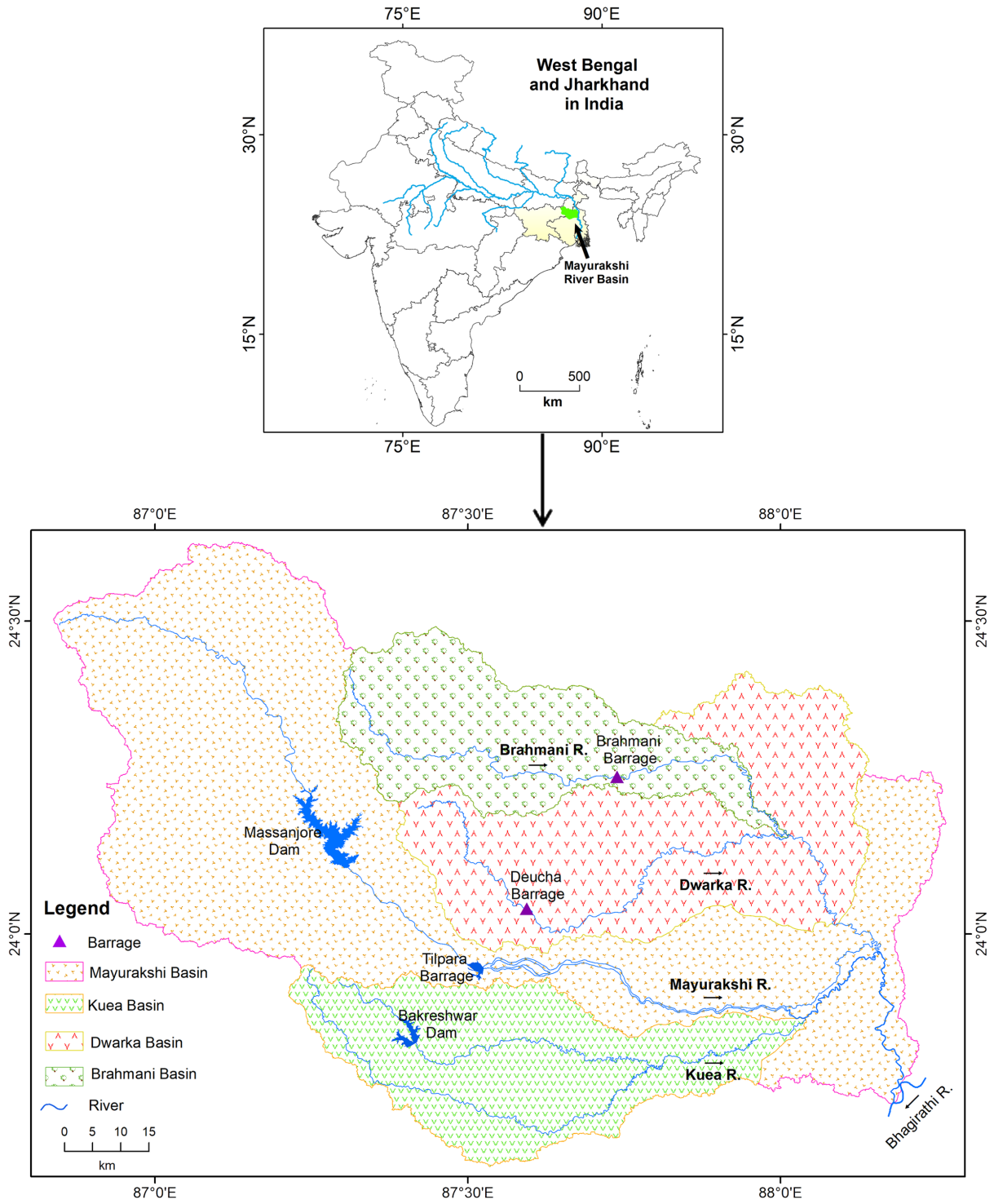

Fig. 1. Location of the monitoring stations over the Mayurakshi system (Note: Bakreshwar dam was initially constructed as Bakreshwar weir)

Citation: Bulletin of Geography. Physical Geography Series 2020, 19, http://dx.doi.org/10.2478/bgeo-2020-0009

Deucha barrage on Dwarka River, Brahmani barrage on Brahmani River, and the Bakreshwar weir on the Kuea River (Fig. 1).

The floods of the lower stretch of the MRB are fascinating. The historicity of floods in 1787 and 1806 is well documented in O'Mally (1914) in district gazetteers. The floods events of 1870, 1885, 1890, 1904, 1907, 1924, 1931, 1932, 1933, 1934, 1951, 1956, 1959, 1961, 1968, 1971, 1978, 1986, 1989, 1992, 1994, 1995, 1996, 1997, 1998, 1999, 2000, 2003, 2004, 2006, 2007, 2013, 2015 as mentioned in *District Disaster Management Plan* prepared by the Office of the District Magistrate (2016) and the *Flood Preparedness and Management Plan* by the Office of the District Magistrate (2014) gives testimony to the severity of flood hazard in the study area. Hence, as per historical records, at least one big flood (inundating about 80% of the study area) has been observed in this tract within a decade. Therefore the frequent and violent floods marginalise agriculture and animal husbandry (Islam and Barman 2020). In a nutshell, the economy of the study area has been paralysed by the severity of flood as well as other socio-cultural processes.

Database and methodology

Database

The Mayurakshi river system consists of four major rivers – the Mayurakshi, the Dwarka, the Kuea and the Brahmani. To assess the frequency and magnitude of the flood of this area, five monitoring stations have been selected: Massanjore dam (24°6'25.22"N, 87°18'32.00"E) for 1978–2009 and Tilpara barrage (23°56'45.55"N, 87°31'30.72"E) for 1957–2009 on the Mayurakshi River, Deucha barrage (24° 2'24.39"N, 87°35'42.11"E) for 1981–2009 on the Dwarka, Brahmani barrage (24°15'4.26"N, 87°44'19.86"E) for 1957–2009 on the Brahmani River and the Bakreshwar weir (23°49'30.43"N, 87°24'54.09"E) for 1956–77 on the Kuea River (Fig. 1). Besides, the major secondary data are comprised of Survey of India topographical maps (1:50,000) and SRTM DEM (30 m), Operational Land Imager or OLI (30 m), District Disaster Report, Murshidabad (2014–16), the district resource maps, climatic data, and soil data. The major databases with their sources are outlined in Table 1.

Table 1. Major databases and their sources

Sl. No.	Database	Sources
1	Peak discharge data at selected monitoring stations	Kandi Master Plan (2012)
2	Topographical maps (72 L-14, 15, 16; 72 P-2,3,4,7,8,11,12,15,16; 73 M-1,5,6,9,10,13,14; 78 D-3, 4; 79 A-1, 2)	Survey of India
3	SRTM DEM (1 Arc-Second Global)	https://earthexplorer.usgs.gov/
4	LANDSAT 5 TM; LANDSAT 8 OLI/TIRS (Path: 139, Row: 43–44)	https://earthexplorer.usgs.gov/
5	District resource maps (Birbhum, Murshidabad and Barddhaman of West Bengal and Devghar, Dumka, Sahibganj and Pakaur of Jharkhand)	Geological Survey of India
6	Climatic data (rainfall)	Worldclim: https://www.worldclim.org/ and India Water Portal http://www.indiawaterportal.org/met_data/
7	Soil data	Chakrabarti (1985)

Methodology

The present study has been carried out using a systematic design of research methodology that starts with the selection of the research problem and study area and ends with the validation of the results with a critical discussion through a chain of processes related to the collection of the data and successful application of the robust methodological algorithms (Fig. 2).

Processing of geo-spatial data and computing slope, drainage density and vegetation density

The drainage basin properties such as relative relief, slope and the drainage density of the study area were extracted from the SRTM DEM (30 m). The DEM is first processed through the fill tools of the Arc toolbox to eliminate the local effects of elevation. The drainage density map was generated from the delineated drainage of the study area using the line density tool in Arc toolbox. The slope map was also prepared from the processed DEM using slope tools of ArcGIS 10.4 software. Similarly, the relative relief map of the study area was prepared using a 1-km^2 grid difference in elevation from DEM using ArcGIS 10.4.

The vegetation density of the present study was computed in a GIS environment using Landsat data. The patches of vegetation cover were traced using the supervised classification by ArcGIS in vector format. The distributions of the vegetation area were extracted into point format per km^2 grid using the fishnet tool in the ArcGIS toolbox. Finally, the IDW interpolation method was applied to depict the distribution of the vegetation density of the study area.

Flood frequency analysis

Flood is a stochastic process, a process partly predictable and partly random (Chow 1988). In Monsoon Asia, the flood is most unpredictable due to the vagaries of the monsoon regime. However, estimating flood frequency and flood magnitude helps

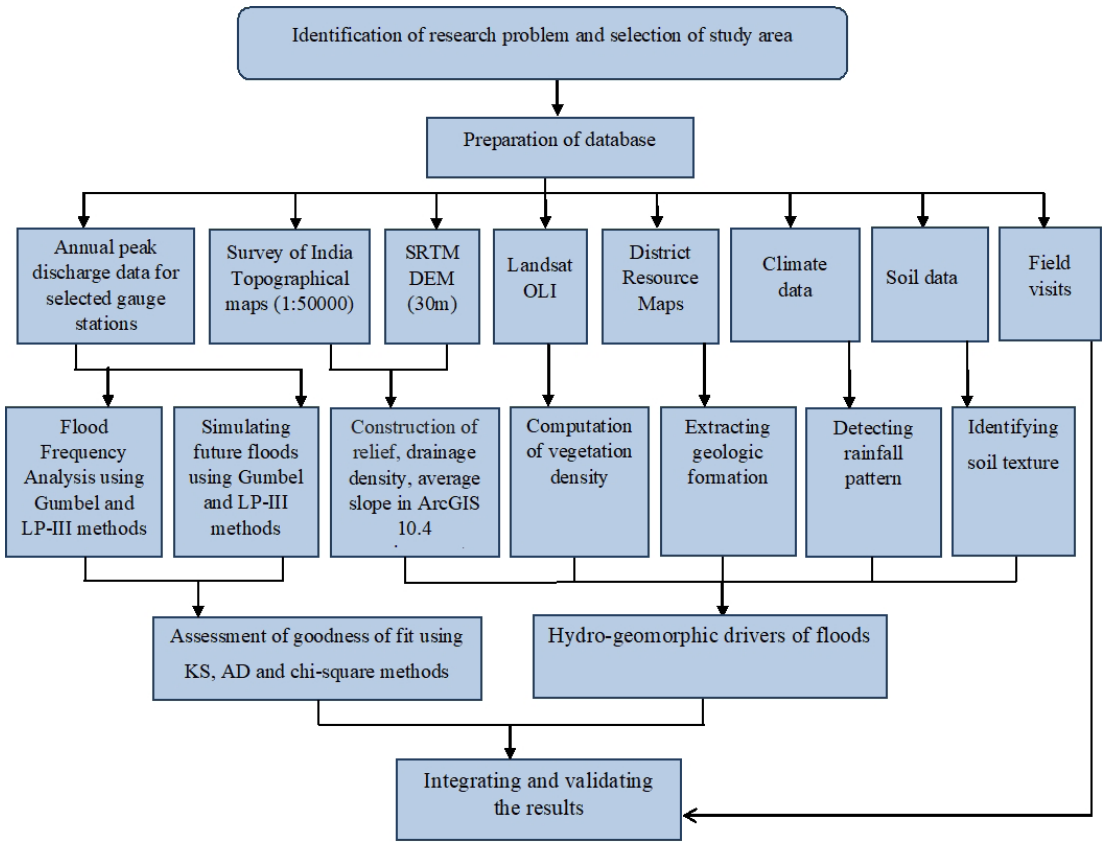

Fig. 2. Flowchart of methodology

Citation: Bulletin of Geography. Physical Geography Series 2020, 19, http://dx.doi.org/10.2478/bgeo-2020-0009

better flood management (Stedinger and Cohn 1986; Stedinger 2007; Stedinger and Griffis 2008; Black and Fadipe 2009; Cunnane 2010; Sarhadi et al. 2012; Rahman et al. 2013; Holmes 2014; Saghafian et al. 2014; Zhang et al. 2014; Sah and Prasad 2015; Kamal et al. 2016; Benameur et al. 2017). However, it is assumed that FFA will be applied successfully if the frequencies follow the normal distribution curve. Therefore, some test statistics including the Mann–Whitney U test are used to detect the normal distribution of the database. Mann–Whitney U Test is a non-parametric test used to identify the nature of distributions – whether their shapes are the same or similar or completely different. In reality, identical distributions are rare. Therefore, to identify the differences in the mean ranks of the two groups, this test is carried out in the present case using IBM SPSS 20. Following Zar (1999), the *U* is computed as follows.

$$U_1 = R_1 - \frac{n_1(n_1+1)}{2} \quad (1)$$

where n_1 stands for the sample size for sample 1, and R_1 for the ranks in sample 1.

As there is no specification which sample is considered Sample 1, an equally valid formula for *U* may be expressed as follows.

$$U_2 = R_2 - \frac{n_2(n_2+1)}{2} \quad (2)$$

The smaller value of U_1 and U_2 is the one used while reading significance tables. The two values are summed as follows.

$$U_1 + U_2 = \mathrm{R1} - \frac{n_1(n_1+1)}{2} + \mathrm{R_2} - \frac{n_2(n_2+1)}{2} \quad (3)$$

Considering $R_1 + R_2 = \mathrm{N}(\mathrm{N}+1)/2$ and n_1+n_2, and performing some algebra, the following may be derived.

$$U_1 + U_2 = n_1 n_2 \quad (4)$$

There are different techniques of probability distribution function for computing the flood frequency and magnitude, such as California method (Barnett 1923), Weinbul (1939), Gumbel (1941, 1958), Chow (1964), Log-Pearson type-III (Bobee and Robitaille 1997), etc. In this work, Gumbel and Log-Pearson type-III distribution functions have been taken into consideration for estimating flood peak with respect to different return periods and probability of occurrence. For computing return period and probability of occurrence flood, the following equations have been used.

$$\mathrm{Tr} = (n+1)/m \quad (5)$$

$$\mathrm{P} = (m/n+1) \quad (6)$$

where, Tr is return period (years), n for the number of observations, m for the rank of the flood magnitude, and P for probability (percent).

Gumbel extreme value method

This method designed by Gumbel (Gumbel 1941) is a well-established probability distribution function used often in hydrological studies for predicting extreme hydrological events, especially for the prediction of maximum expected rainfall and flood peak (Yue et al. 1999). In the Gumbel method, the expected maximum discharge (X_T) of the different return period (T) and the probability of exceedance (P) is calculated using the following algorithm.

$$X_T = \overline{X} + K_T\delta \quad (7)$$

where, X_T = the maximum value of expected rainfall, $\overline{x}$ = mean rainfall, δ = standard deviation and K_T = frequency factor which is calculated using the following formula.

$$K_T = Y_T - \overline{y}/\delta \quad (8)$$

where Y_T = reduced variate, $\overline{Y}$ = mean of reduced variate and δ = standard deviation of reduced variate. Reduced variate is calculated using the following equation.

$$Y_T = -(ln.\left(ln\frac{T_r}{T_r-1}\right)) \quad (9)$$

The reduced variate is used to establish whether the observed flood data follows the Gumbel distribution or not. If the plot of the reduced variate and flood peak follows a linear pattern, it can be concluded that the Gumbel distribution fits well with the observed data.

Log-Pearson Type III

This method involves some calculation steps that provide the maximum value of expected discharge (X_T) with respect to every return period (Tr) and the probability of exceedance (P). In the very first step, hydrological data are transformed to logarithms with base 10 (y=log x). Then, based on the logarithmic data, the mean ($\overline{x}$), standard deviation (δ) and coefficient of skewness (Cs) are computed.

Again, based on the value of the coefficient of skewness (Cs) and the return period (Tr) frequency factor (K_T) is calculated. By principle, when Cs is equal to zero (Cs=0), it determines that the frequency factor is equal to a standard normal variable (z) which is calculated using the following formula.

$$z = w - \frac{2.515517+0.802853w+0.0110328w^2}{1+1.432788w+0.189269w^2+0.001308w^3} \quad (10)$$

where w is calculated using the following expression.

$$w = \left\{\ln\left(\frac{1}{p^2}\right)\right\}^{1/2} \quad (0 < p \leq 0.50) \quad (11)$$

where w is the exceeding probability (p=1/T), w is intermediate variable when p> 0.5, *1-p* is substituted for p in above equation.

But when Cs is not equal to zero, the frequency factor (KT) is calculated using the following equation.

$$K_T = Z + (Z^2-1)K + \frac{1}{3}(Z^3-6Z)K^2 - (Z^2-1)K^3 + ZK^4 + \frac{1}{3}K^5 \quad (12)$$

where, $k = \frac{C_s}{6}$

Finally, the expected discharge is calculated putting all the variables in the following equations.

$$X_T = Antilog\ \overline{X} \quad (13)$$

$$Log\ X = \overline{X} + K_T\delta \quad (14)$$

where, X_T = the maximum value of expected rainfall, $\overline{x}$ = mean rainfall, δ = standard deviation and K_T = frequency factor.

Computation of confidence limits

The confidence limit shows an interval within which the population value of the mean falls with some probability (Mahmood 1977). In the context of finding thresholds of discharge that may induce floods in the MRB, the confidence limits were computed at 95% and 99% level as follows.

$$\overline{x} - \frac{3\sigma}{\sqrt{n}} \text{ to } \overline{x} + \frac{3\sigma}{\sqrt{n}} \quad \text{for 99\% confidence limit (15)}$$

$$\overline{x} - \frac{2\sigma}{\sqrt{n}} \text{ to } \overline{x} + \frac{2\sigma}{\sqrt{n}} \quad \text{for 95\% confidence limit (16)}$$

where, stands for mean of the random sample, for standard deviations of the population, and n for sample size.

Goodness of fit

The probability distribution implies a certain degree of uncertainty. Therefore, any simulation using the probability function needs testing of the goodness of fit. There are different tests such as Kolmogorov–Smirnov (KS), Thapiro–Wilk (TW), Anderson–Darling (AD), x^2 distribution, Mean Standard Error (MSE) used by the previous scholars in FFA. The test results confer relative acceptance of the results rather than the rejection of the probability function (Millington et al. 2011). In the present context, we have employed Kolmogorov–Smirnov (KS), Anderson–Darling (AD), and x^2 distribution.

The Kolmogorov–Smirnov (KS) test statistic takes the consideration of the largest vertical distance ($^{sup}_{x}$) from empirical and theoretical cumulative density function. Thus, it is computed using the following expression.

$$D = \sup_x |F_e(x) - F_o(x)| \quad (17)$$

where, D - maximum additional deviations among the two distributions, Fe(x) - the cumulative distribution function of the theoretical distribution, Fo(x) - the empirical distribution function of observed data.

The Anderson–Darling (AD) test considers the difference between the observed cumulative distribution function (CDF) and theoretical CDF with an emphasis on the tail of the distribution. This enables the researchers to find any outliers in the distribution. The AD statistic (A2) may be computed using the following formula (McCuen 1993). If the AD statistic is more than the critical value at a certain significance level, the test hypothesis is rejected, implying the improbability of the distribution.

$$A2 = n - \frac{1}{n}\sum_{i=1}^{n}(2i-1).[\ln F(Xi) + \ln(1 - F(Xn-i+1))] \quad (18)$$

where F = cumulative distribution function, Xi = ordered observed data.

Karl Pearson (1916) proposed the use of x^2 distribution for the goodness of the fit of the results computed. It compares the observed data with expected data using the following algorithm.

$$x2 = \sum_{j=1}^{n}\left(\frac{oj\,(Ql) - Ej(Q))2}{Ej\,(Q)}\right) \quad (19)$$

where, *Oj (Q)* and *Ej (Q)* = observed frequency and expected frequency of the j^{th} class respectively, n = number of classes.

Citation: Bulletin of Geography. Physical Geography Series 2020, 19, http://dx.doi.org/10.2478/bgeo-2020-0009

Results

Nature of floods

Flood is the most frequently occurring natural hazard in the lower stretch of the MRB, especially in the Rarh tract of West Bengal. The annual hydrographs of the gauge stations of the MRB portray that annual flood peaks are concentrated in the monsoon months. However, it is noteworthy that annual flood peaks are shifting from August (pre-dam condition) to September (post-dam condition) as depicted by Tilpara barrage (Ghosh and Pal 2015). The historic floods of 1870, 1885, and 1890 were the results of the breaching of the embankment of Lolitakuri of Bhagwangola –II. Similarly, in the last century (1920–2019), there were 25 major floods documented in the District Disaster Management Plan, Murshidabad (2016–17). About 48% of the total floods are triggered by the Ganga-Padma system, while about 16% of floods are triggered by the Mayurakshi River. When the two river systems (Ganga-Padma and Mayurakshi) merge together, big floods occur (District Disaster Report, Murshidabad 2016–17). About 36% of floods of this kind devastated almost the whole district and induced huge devastation of human life, animals and crops. For example, Kandi Subdivision suffered heavy losses during the floods of 1931–32; the destruction of five thousand houses in the Rarh area and eight thousand people were affected during 1933–34. The flood-affected one third of the area (4920 km^2) of the entire district during 1968, including 845 villages spread over an area of nearly 1255 km^2. Out of 26 Community Development (CD) blocks of the district, 21 were flooded and it affected 820,000 persons. Furthermore, 52,000 houses were destroyed and crops spread over 80,935 hectares of land worth 100 million rupees were damaged during 1978. Besides, Kandi Subdivision was heavily affected, along with seven community development (CD) blocks from Farakka to Jalangi (1,850 km^2) being partially affected. A total of 2.3 million persons were affected (13 people died) in the six municipalities and 221 Gram Panchayats (cluster of villages). Moreover, 70,200 houses were completely damaged and 89,000 houses were partially damaged. The 26 CD blocks suffered monetary loss of INR 5.61 billion during 1999; 600 human lives were lost and pecuniary loss exceeded INR 20 billion during the colossal flood of 18–21 September 2000. During that period, 79,912 people were affected and 22,746 houses were damaged. The district of Murshidabad suffered damage to crops, estimated value of which was INR 974.5 billion. Besides, two lives were lost during 2004. During 2006, flood inundated almost 1,892 villages and seven municipalities over 26 CD blocks, with 1,436,334 people affected and 35,437 houses fully and 50,729 partly damaged. Besides, it resulted in damages to 74,476 hectares of land and claimed 11 lives. During 2007, 556,995 persons were affected including the loss of 20 human lives in the 1,310 villages and seven municipalities spread over the 26 CD blocks. Similarly, the flood of 2015 badly affected 250,000 people including the loss of five human lives in 84 Gram Panchayats of the 14 blocks and one municipality (District Disaster Report, Murshidabad 2016–17). As per the historical records, the largest flood since 1860 is the colossal flood of 2000, which affected an area of about 1,393 km^2 of the MRB (Islam and Barman 2020). Due to the recurrent floods in the MRB, buildings are dilapidated (Fig. 3a, b), crops go underwater (Fig. 3c) and the transportation system is disrupted (Fig. 3d).

Flood frequency and magnitude

Flood frequency analysis (FFA) is basically performed with the help of statistical measures for getting sophisticated ideas on the hydrological behaviour of a river. Before we examine the nature of flood frequency and magnitude, it is necessary to state the nature of the peak discharge data using the Mann–Whitney U test (Table 2). The results show that all the distributions have little perturbations except for Massanjore. However, the two groups of each monitoring station have no significant statistical differences, i.e. the null hypothesis is accepted at 0.05 significance level for Massanjore, Deucha and Bakreshwar stations, while Tilpara and Brahmani have rejected the null hypothesis at 0.05 significance level but retained null at different significance levels (Table 2). This portrays that the discharge data is competent for further analysis. Therefore, in the present context, to portray the nature and dy-

Fig. 3. Severity of flood, a. and b. Dilapidated kutcha (muddy/thatched) houses due to flood in Hijal, Murshidabad c. Inundated land in Hijal d. Breaching of the pakka (concrete) road by flood (Source: Field photographs 2018)

namics of the flood, peak discharge and associated descriptive statistics are used along with the probability density functions and threshold discharges as discussed in the following sections.

For Massanjore the maximum flood peak recorded was in the year 1991 (8,980 $m^3 s^{-1}$), followed by 1992 (7570 $m^3 s^{-1}$), 1987 (5690 $m^3 s^{-1}$). In recent times, a flood peak of about 3,260 $m^3 s^{-1}$ was recorded in 2004 (Fig. 4a). Similarly, the Tilpara barrage exhibited the highest flood peak of about 11,330 $m^3 s^{-1}$ in 1978 followed by a peak of 7,430 $m^3 s^{-1}$ in the year 2000. Besides, another major peak (6,680 $m^3 s^{-1}$) was noted in the year 1959 (Fig. 4b). The pattern of annual peak discharge of the Brahmani River is different from the Mayurakshi River, where an oscillatory graph was recorded with the highest flood peak of about 1,950 $m^3 s^{-1}$ in the year 2000. Another peak of about 1,750 $m^3 s^{-1}$ was noted for 1990 and about

Citation: Bulletin of Geography. Physical Geography Series 2020, 19, http://dx.doi.org/10.2478/bgeo-2020-0009

Table 2. Mann–Whitney U test

Monitoring stations	Ranks				Test Statistics				Remarks
	Group	N	Mean Rank	Sum of rank	Mann–Whitney U	Wilcoxon W	Z	Asymp. Sig. (2-tailed)	
Massanjore	pre-1993	16	16.5	264	128	264	0	1	Retain null hypothesis at 0.05 significance level
	post-1993	16	16.5	264					
Tilpara	pre-1982	26	20.58	535	184	535	-2.971	0.003	Retain null hypothesis at 0.001 significance level
	post-1982	27	33.19	896					
Brahmani	pre-1982	26	22.04	573	222	573	-2.295	0.022	Retain null hypothesis at 0.01 significance level
	post-1982	27	31.78	858					
Deucha	pre-1994	14	12.07	169	64	169	-1.79	0.73	Retain null hypothesis at 0.05 significance level
	post-1994	15	17.73	266					
Bakreshwar	pre-1966	10	12.4	124	41	107	-0.986	0.324	Retain null hypothesis at 0.05 significance level
	post-1966	11	9.73	107					

1,550 $m^3 s^{-1}$ was recorded for 1978 (Fig. 4c). Besides, the Dwarka River exhibited the highest flood peak of about 1,270 $m^3 s^{-1}$ in 2000 at Deucha barrage (Fig. 4d). Due to the unavailability of data on Kuea River in recent times the frequency-magnitude analysis is restricted to the year 1977. From this small period of data, it is observed that about 710 $m^3 s^{-1}$ was recorded as the highest peak discharge. Another similar peak was also noted in the following year 1959 (Fig. 4e). It has been observed that the majority of the flood contribution comes from the Mayurakshi River mainly from the discharge of the Tilpara barrage. Thus, this analysis detected the years of 1978 and 2000 as the two major flood episodes in history. It is worth mentioning that after 2000 there were no such large floods. However, the five-year moving average portrayed that there is a rising trend of flood peaks for both the Mayurakshi and Brahmani River. Similarly, a slight rising trend is also observed for the Dwarka River (Fig. 4a–e). The analysis therefore involves the computation of some statistical attributes such as mean, standard deviations and skewness coefficient of the observed annual peak flow discharge. The results portray that Tilpara barrage records the highest average discharge (1,572 $m^3 s^{-1}$), highest range (11,303 $m^3 s^{-1}$), highest standard deviation (2,175 $m^3 s^{-1}$), highest IQR (1,045 $m^3 s^{-1}$) and highest median (873 $m^3 s^{-1}$), while the Bakreshwar weir has the record of lowest average discharge, range, SD and median (Table 3). Therefore, the statistical measures depict that the variability of flood discharge is significantly higher in the Mayurakshi River than in the other rivers (Fig. 5f).

Furthermore, the probability density function (PDF) shows similar results. Massanjore and Tilpara have a highly skewed distribution, where the maximum percentage of the distribution area is concentrated at the lower end of the continuum. For Massanjore, about 75% of the PDF is concentrated within the peak discharge of 1,500 $m^3 s^{-1}$ while the same percentage of the PDF has been found within the limit of 2,000 $m^3 s^{-1}$ (Fig. 5a, b). This shows

Table 3. Descriptive statistics of the flood discharge

	Observation period	Average ($m^3 s^{-1}$)	Range ($m^3 s^{-1}$)	Standard deviation ($m^3 s^{-1}$)	Coefficient of skewness	IQR ($m^3 s^{-1}$)	Median ($m^3 s^{-1}$)
Massanjore dam	1978–2009	1,438	8,980–57	2,139	2.28	1,025	614
Tilpara barrage	1957–2009	1,572	11,327–24	2,175	2.50	1,045	873
Brahmani barrage	1981–2009	792	19,54–110	473	0.50	720	684
Deucha barrage	1957–2009	372	1,264–82	236	1.64	254	356
Bakreshwar weir	1956–1977	238	708–34	219	0.86	328	118

Computed by the authors

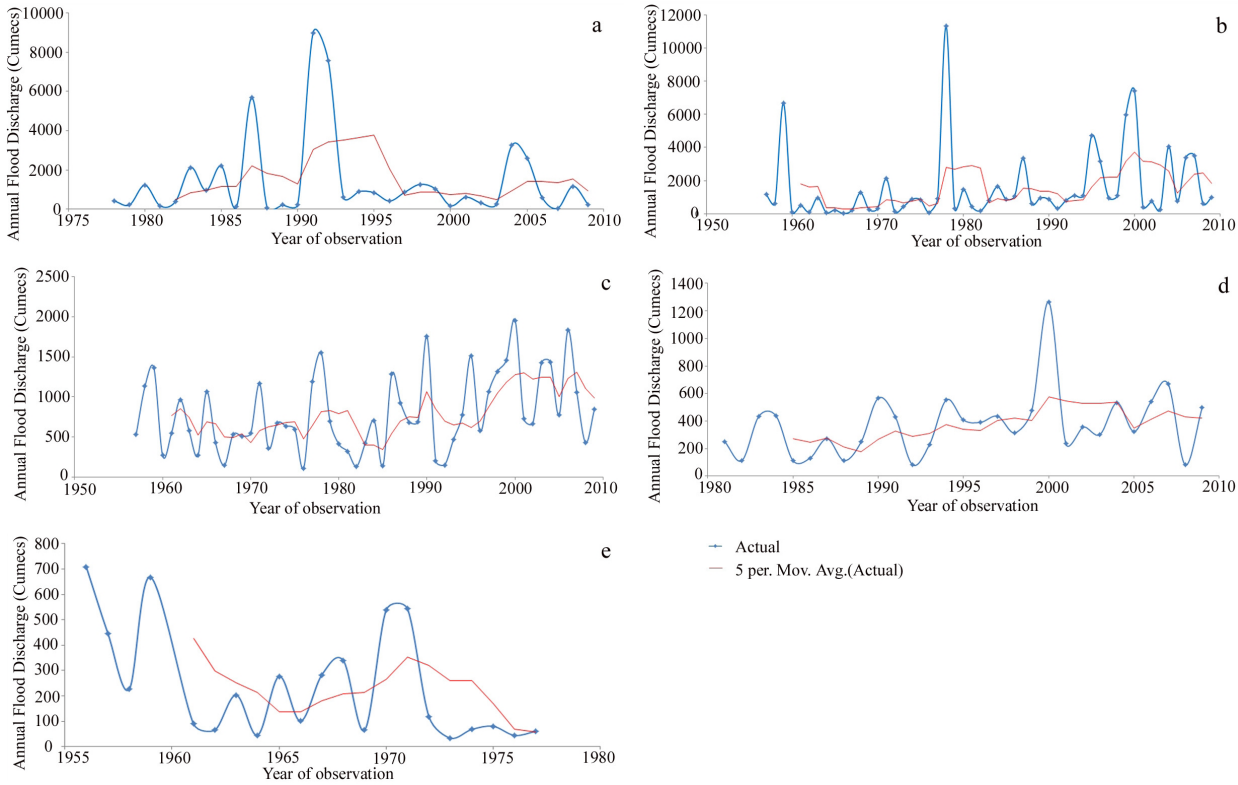

Fig. 4. Annual flood discharge a. Massanjore dam, b.Tilapara barrage, c. Brahmani barrage, d. Duecha Barrage, e. Bakreshwar weir (Source: Kandi Final Report 2012)

the frequent low magnitude flood and very occasional medium- to high-magnitude flood. However, the Brahmani River has more normally distributed functions, with the highest percentage of the PDF in the middle of the distribution (Fig. 5c). Similarly, the Dwarka River (Deucha barrage) and Kuea River (Bakreshwar weir) have skewed distribution but not as high as the Mayurakshi River (Fig. 5d, e). This proves that the larger the river the greater the deviation from the normal distribution (Fig. 5a–e). The curves fitted with the Gumbel and Log-Pearson type III also show this fluctuating nature of the river regime, especially for the Mayurakshi River. The geometry of the curves depicts that LP-III has a more peaked (leptokurtic) distribution than Gumbel for all the monitoring stations except Brahmani River (Fig. 5a–e).

It is noteworthy that probability density function can provide information only about the concentration of frequencies around a maximum probability of discharges, but not about the threshold or critical limit of discharge. Moreover, not all annual peak discharges can generate floods. Therefore, the critical discharg-

Citation: Bulletin of Geography. Physical Geography Series 2020, 19, http://dx.doi.org/10.2478/bgeo-2020-0009

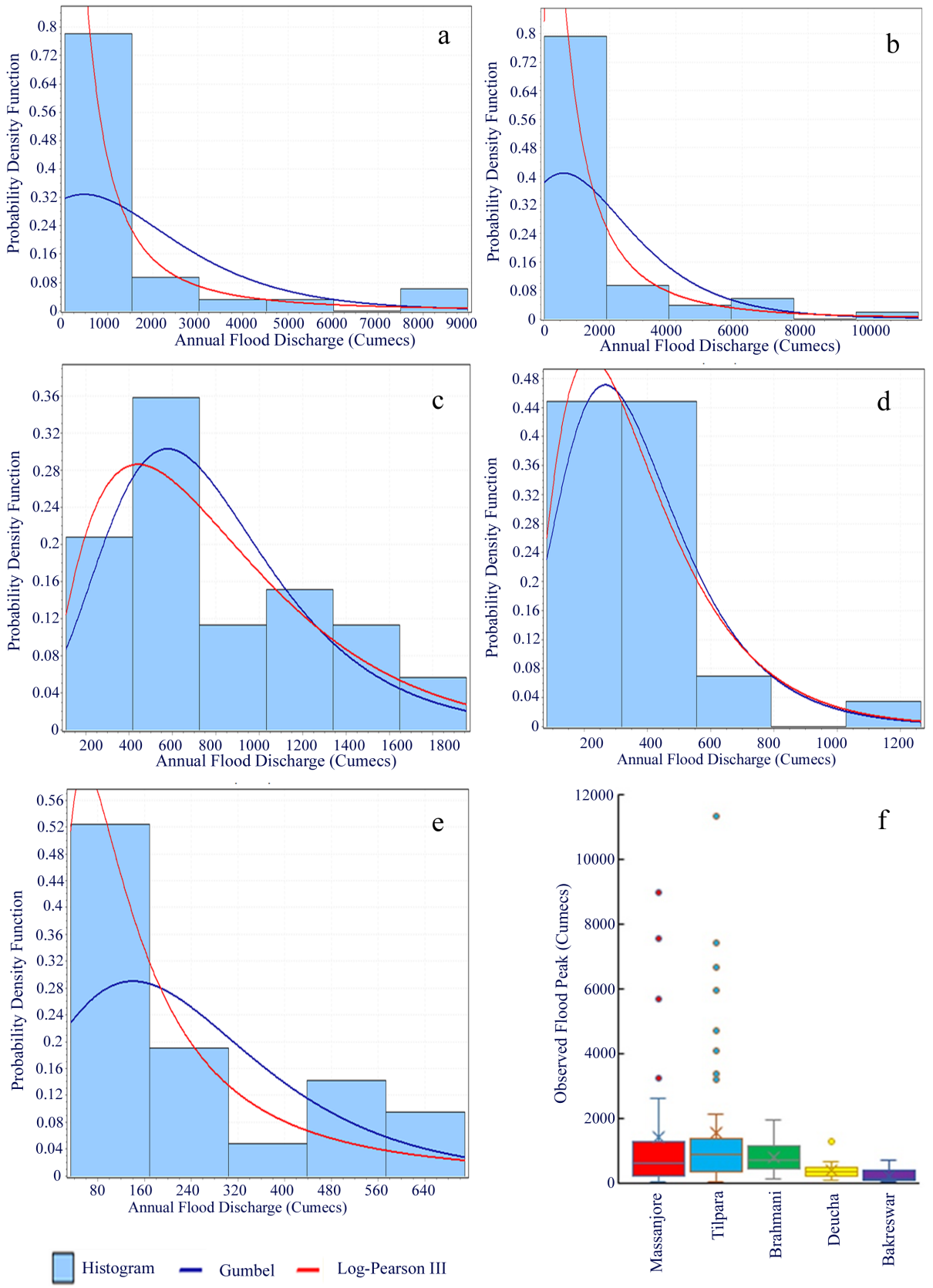

Fig. 5. Probability density function (a. Massanjore, b. Tilpara, c. Brahmani, d. Deucha, e. Bakreshwar) and f. box plot showing variation of flood discharge

es of rivers that may produce floods downstream have been computed at 95% and 99% confidence limit (Table 4). At the 95% confidence limit, a threshold discharge of 681.54 m^3 s^{-1} may produce a small magnitude flood, while 2,194.61 m^3 s^{-1} may produce large floods at Massanjore. However, at the 99% confidence limit, a lower magnitude threshold (303.27 m^3 s^{-1}) is recorded at the lower limit while a higher magnitude threshold (2572.87 m^3 s^{-1}) is noted at the upper limit (Table 4). Similarly, other monitoring stations also exhibit a typical threshold to generate floods in the respective stations.

Observed flood magnitude against different return periods and probability

Computing the return period for a specified flood magnitude is based on the historical data to indicate flood probability and risk analysis of a particular region. Regarding Massanjore, during the last 32 years, the maximum peak discharge recorded was about 8,980 m^3 s^{-1} with a return period (Tr) of 33 years and a probability (P) of about 3%. Similarly, the flood similar to the magnitude of about 7,570 m^3 s^{-1} (1992) and 5,687 m^3 s^{-1} (1987) would recur after 16.5 years and 11 years with probabilities of about 6% and 9% respectively. Thus, the lesser the flood magnitude, the higher the flood probability (Tingsanchali and Karim 2010; Keast and Ellison 2013). During the last 32 years, the minimum peak discharge recorded was about 57 m^3 s^{-1} in 2007 (Tr=1.03, P=96.96). The peak discharge of this magnitude would recur almost every year with a probability of about 97%. Among the 53 years of observation of Tilpara, the year 1978 registered the highest flood peak of 11,326 (Tr=54, P=1.85%), while the minimum peak discharge is found to be 24 in 1966 (Tr=1.01, P=98.14). The average peak discharge during this period is observed as 1,572 m^3 s^{-1} with a high standard deviation of 2,175 m^3 s^{-1}. Among the total observation, 22% (n=12) were above the average peak discharge, where the minimum peak discharge has been found as 2,123 m^3 s^{-1} with a return period of 4.90 years and a probability of about 20.37%. Similarly, the maximum peak discharge among the 53 years of Brahmani, was recorded as 1,953 m^3 s^{-1} in 2000 (Tr=54, P=1.85) and lowest as 110 m^3 s^{-1} in 1976 (Tr=1.01, P=98.14) while the average peak discharge and standard deviation are 792 m^3 s^{-1} and 473 m^3 s^{-1}, respectively. Regarding Deucha, the maximum and minimum peak discharge were recorded as 1,264 m^3 s^{-1} in 2000 (Tr=30, P=3.33) and 82 in 2008 (Tr=1.03, P=96.66), respectively, while the average and standard deviation were found to be 372 m^3 s^{-1} and 236 m^3 s^{-1}, respectively. Regarding Bakreshwar, the maximum peak discharge was recorded as 707 m^3 s^{-1} in 1956 (Tr=22, P=4.55). The peak discharge close to the highest magnitude is about 668 m^3 s^{-1} (1959), which would recur after 11 years at a probability of about 9%, while the minimum peak discharge is found to be 33 m^3 s^{-1} having 1.05 recurrence intervals with a probability of about 95%.

Simulating future flood of the different return periods

It is well recommended and accepted that projecting the expected flood discharge for 2- to 200-year return periods is sufficient for developing flood mit-

Table 4. Thresholds of flood discharges (m^3 s^{-1}) at 95% and 99% confidence limits

Monitoring stations	95% confidence limit		99% confidence limit	
	Lower limit (m^3 s^{-1})	Upper limit (m^3 s^{-1})	Lower limit (m^3 s^{-1})	Upper limit (m^3 s^{-1})
Massanjore	681.54	2,194.61	303.27	2,572.87
Tilpara	974.77	2,170.27	675.90	2,469.14
Brahmani	661.17	924.09	595.44	989.82
Deucha	284.73	460.68	240.74	504.66
Bakreshwar	142.81	334.44	94.90	382.34

 Citation: Bulletin of Geography. Physical Geography Series 2020, 19, http://dx.doi.org/10.2478/bgeo-2020-0009

igation strategies that help people to cope with flood risk and vulnerability (Khan and Iqbal 2013). Therefore, the forecasting of expected maximum flood peak has been computed for different return periods (2, 5, 10, 25, 50, 100 and 200 years). The expected flood discharge corresponding to return periods were derived from the Gumbel and LP-III distribution for five gauge stations (Massanjore, Tilpara, Brahmani, Deucha, and Bakreshwar). In the case of Massanjore, the estimated flood discharge for 2-year return periods are 1,110 $m^3 s^{-1}$ using Gumbel and 625 $m^3 s^{-1}$ using LP-III, while for the 200-year return period flood discharge records 10,533 $m^3 s^{-1}$ using Gumbel and 22,942 $m^3 s^{-1}$ using LP-III (Table 5). Regarding Tilpara, for a 2-year return period, it is 1,833 $m^3 s^{-1}$ using Gumbel and 813 $m^3 s^{-1}$ using LP-III while for a 200-year return period simulated discharge is 11,033 $m^3 s^{-1}$ using Gumbel and 14,179 $m^3 s^{-1}$ using LP-III (Table 6). For Brahmani, against a 2-year return period, it is 718 $m^3 s^{-1}$ using Gumbel (Table 5) and 684 $m^3 s^{-1}$ using LP-III (Table 6), while it is 2,720 (Gumbel) and 2,758 (LP-III) for the 200-year return period. Similarly, for Deucha, it is 336 $m^3 s^{-1}$ (Gumbel), 322 $m^3 s^{-1}$ (LP-III) for the 2-year period, while it is 1,389 $m^3 s^{-1}$ (Gumbel) and 1,303 $m^3 s^{-1}$ (LP-III) for the 200-year return period. For Bakreshwar, it is 206 $m^3 s^{-1}$ (Gumbel) and 148 $m^3 s^{-1}$ (LP-III) while it is 1,213 $m^3 s^{-1}$ (Gumbel) and 2,383 $m^3 s^{-1}$ (LP-III) for the 200-year return period (Table 6).

Goodness of fit

The expected discharge computed using the extreme value method of Gumbel and the Log-Pearson III shows that there is a variation in the results. Therefore, the goodness of fit is essential towards the relative acceptance and reliability of the results. Thus, graphical fitting of the expected discharge to the observed data on quantile-quantile (Q-Q) plot shows that all the distributions are deviated from normal because normally distributed points will fall on the 1:1 line (Bhat et al. 2019). Thus, they have some skewness (Fig. 6a–e). In the present study, both the Massanjore and Tilpara over the Mayurakshi River recorded more skewness for Gumbel than for LP-III. Similar observations have been traced out for the other stations, including Deucha and Bakreshwar. However, there is no such difference between the Gumbel method and LP-III (Fig. 6d, e). Moreover, the Brahmani barrage has less skewness for both the LP-III and Gumbel method and tends to be normally distributed (Fig. 6c). However, to ascertain the nature of expected data to normal distribution, the Kolmogorov–Smirnov (KS), Anderson–Darling (AD) and chi-squared test statistics add some significant insights. For example, all the monitoring stations tend to be normal regarding the expected discharge computed using the Gumbel method and LP-III methods, as reflected by the lower test statis-

Table 5. Expected flood discharge at different return periods using Gumbel method

Return period	Probability (%)	yt	Massanjore		Tilpara		Brahmani		Deucha		Bakreshwar	
			kt (Frequency factor)	xt (Discharge $m^3 s^{-1}$)	kt (Frequency factor)	xt (Discharge $m^3 s^{-1}$)	kt (Frequency factor)	xt (Discharge $m^3 s^{-1}$)	kt (Frequency factor)	xt (Discharge $m^3 s^{-1}$)	kt Frequency factor)	xt (Discharge $m^3 s^{-1}$)
2	50	0.367	-0.153	1,110	-0.157	1,834	-0.157	718	-0.152	337	-0.148	206
5	20	1.500	0.859	3,277	0.815	3,949	0.815	1,179	0.870	579	0.906	438
10	10	2.250	1.530	4,712	1.459	5,350	1.459	1,483	1.547	739	1.604	591
25	4	3.199	2.377	6,524	2.272	7,120	2.272	1,868	2.402	942	2.486	784
50	2	3.902	3.005	7,869	2.875	8,432	2.875	2,154	3.037	1,092	3.140	928
100	1	4.600	3.629	9,204	3.474	9,736	3.474	2,438	3.667	1,241	3.789	1,070
200	0.5	5.296	4.251	10,534	4.071	11,034	4.071	2,720	4.294	1,390	4.436	1,213

Computed by the authors

Table 6. Expected flood discharge at different return periods using LP-III method

Return period	Probability (%)	Massanjore		Tilpara		Brahmani		Deucha		Bakreshwar	
		kt (Frequency factor)	xt (Discharge $m^3 s^{-1}$)	kt (Frequency factor)	xt (Discharge $m^3 s^{-1}$)	kt (Frequency factor)	xt (Discharge $m^3 s^{-1}$)	kt (Frequency factor)	xt (Discharge $m^3 s^{-1}$)	kt (Frequency factor)	xt (Discharge $m^3 s^{-1}$)
2	50	-0.0465	625	0.049	813	0.100	684	0.072	322.14	-0.0343	148
5	20	0.825	1858	0.853	2255	0.857	1188	0.855	543.19	0.8295	349
10	10	1.307	3394	1.246	3715	1.199	1525.52	1.225	695.34	1.3017	557
25	4	1.842	6624	1.646	6171	1.526	1936	1.592	887.77	1.8206	931
50	2	2.201	10357	1.895	8458	1.718	2225	1.813	1029.08	2.1632	1307
100	1	2.529	15620	2.110	11118	1.877	2499	2.002	1167.19	2.4778	1784
200	0.5	2.837	22942	2.302	14179	2.012	2758	2.167	1303.04	2.7704	2383

Computed by the authors

tic of the KS, AD and chi-squared test compared to the critical value at 0.01 level (Tables 7–9). However, the Tilpara barrage over the Mayurakshi River has a significant difference between the theoretical distribution and empirical distribution, as reflected by the higher computed value of the Gumbel compared to the critical value at the 0.01 significance level. Thus, the distribution of the Tilpara indicates that the "alternative" hypothesis is accepted due to the significant variation in the annual discharge. This may happen due to the huge basin area above Tilpara that involves the typical peninsular rainfall regime (Ghosh 2003). Moreover, the tests suggest that the LP-III method is more reliable in simulating floods than the Gumbel method (Tables 7–9).

5. Discussions

The FFA shows that the monitoring stations such as Massanjore and Tilpara on the large river, i.e. the main Mayurakshi River compared to the monitoring stations (Deucha, Brahmani and Bakreshwar) located on the tributaries in the MRB are found to record a large degree of variability of the annual peak discharge due to higher catchment areas, greater hydro-geomorphic diversity and other anthropogenic controls. The catchment areas for Massanjore, Tilpara, Bakreshwar, Dwarka, and Brahmani are 1,859 km^2, 3,208 km^2, 142.45 km^2, 303.03 km^2 and 688.94 km^2, respectively, as per the estimate of Irrigation and Waterways Dept., Govt. of West Bengal.

Futhermore, Tilpara is the only gauge station that exhibits a strong variable nature of flood peak. This may be due to the frequent release of water from the upstream Massanjore dam in both the lean and monsoon season. During the monsoon, due to the lowering of the live storage capacity of the Massanjore dam at the siltation rate of 1.617 mcm/year (World Commission on Dams 2000) water is released, while in the winter season water release is intended for *rabi* cultivation (Dasgupta 2001). This problem further aggravates when the three main tributaries between Massanjore and Tilpara, namely the Kushkarani River, Siddheswari River and Ghoshbera River, add substantial monsoon discharge. For example, Kushkarani River and Siddheswari River contribute 105.66 $m^3 s^{-1}$ and 43.91 $m^3 s^{-1}$, respectively, during the monsoon (Islam and Barman 2020).

Another significant observation is that the Q-Q plot shows that Brahmani Barrage and Deucha Barrage have similar FFA results of Gumbel and LP-III, but others do not. This may be due to the location of Brahmani Barrage and Deucha Barrage in an almost homogeneous group located in the north-eastern part of the MRB controlled by a uniform slope and northern irrigation canal system that contributes a regular flow to this system from Tilpara bar-

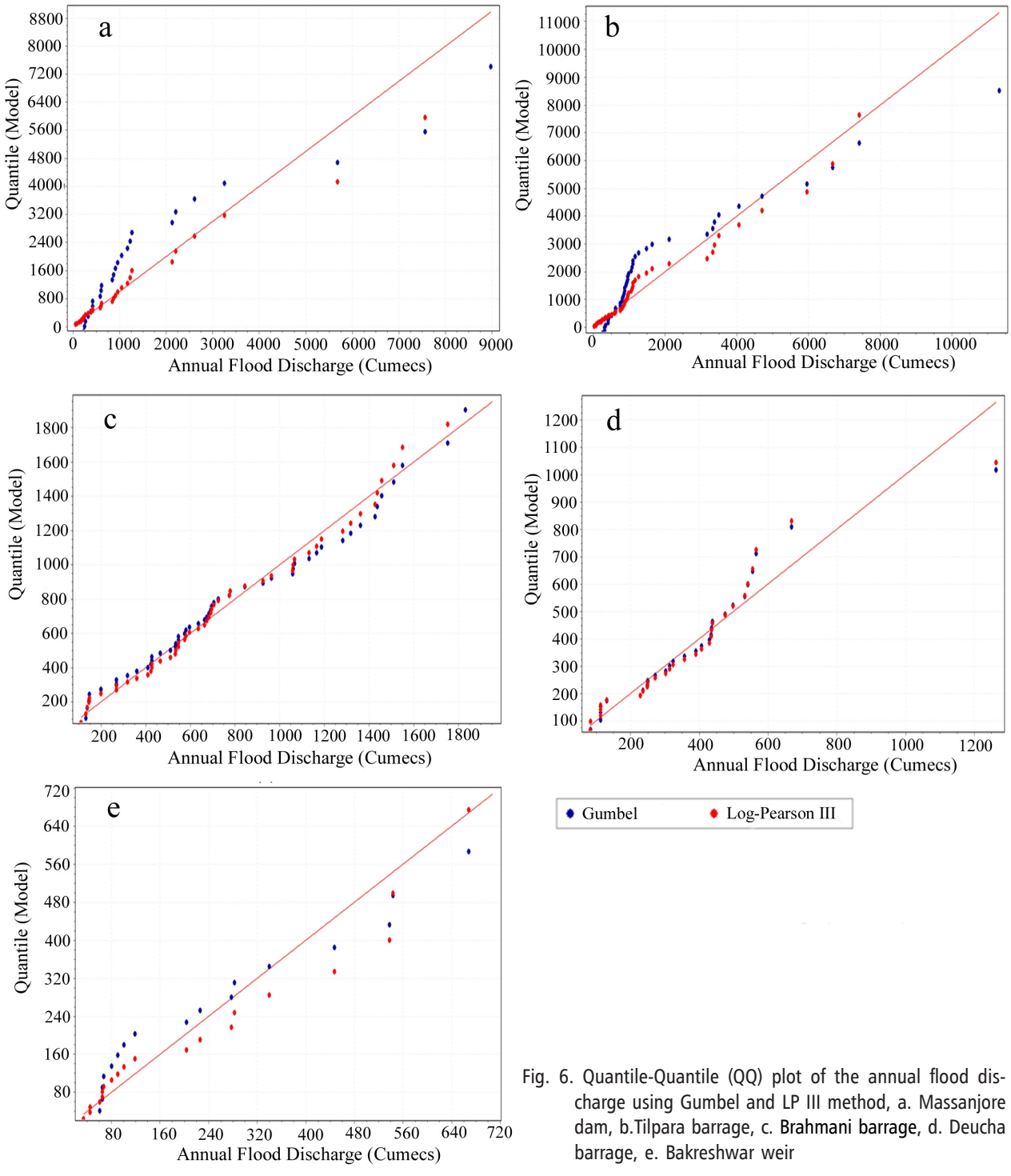

Fig. 6. Quantile-Quantile (QQ) plot of the annual flood discharge using Gumbel and LP III method, a. Massanjore dam, b.Tilpara barrage, c. Brahmani barrage, d. Deucha barrage, e. Bakreshwar weir

rage (Dasgupta 2001). However, Bakreshwar weir in the southern part of the MRB showed a relatively higher fluctuation due to the presence of the then semi-controlled weir structure installed during 1928–30 that could only partially control the flow during the monsoon period.

Moreover, each system behaves differently owing to some controlling factors. Thus, these peculiarities of the FFA of the MRB need to be addressed from the perspective of hydro-geomorphic and anthropogenic controls of the flood.

Table 7. Kolmogorov–Smirnov tests of normality

Monitoring stations	Methods	Kolmogorov–Smirnov						
		Sample size	Statistic	Significance level	Critical value	P value	Reject	Rank
Massanjore	Gumbel	32	0.27663	0.01	0.28094	0.01175	No	39
	LP-III	32	0.07126	0.01	0.28094	0.99307	No	3
Tilpara	Gumbel	53	0.24693	0.01	0.21968	0.00248	Yes	38
	LP-III	53	0.11500	0.01	0.21968	0.15149	No	13
Brahmnai	Gumbel	53	0.08074	0.01	0.21968	0.85244	No	18
	LP-III	53	0.06171	0.01	0.21968	0.98015	No	1
Deucha	Gumbel	29	0.10967	0.01	0.29466	0.83940	No	12
	LP-III	29	0.11143	0.01	0.29466	0.82561	No	17
Bakreshwar	Gumbel	21	0.20071	0.01	0.34427	0.32165	No	33
	LP-III	21	0.13245	0.01	0.34427	0.80891	No	9

Computed by the authors

Table 8. Anderson–Darling tests of normality

Monitoring stations	Methods	Anderson–Darling					
		Sample size	Statistic	Significance level	Critical value	Reject	Rank
Massanjore	Gumbel	32	3.19450	0.01	3.9074	No	31
	LP-III	32	0.16678	0.01	3.9074	No	3
Tilpara	Gumbel	53	4.69740	0.01	3.9074	Yes	31
	LP-III	53	0.51526	0.01	3.9074	No	10
Brahmnai	Gumbel	53	0.45088	0.01	3.9074	No	18
	LP-III	53	0.32399	0.01	3.9074	No	3
Deucha	Gumbel	29	0.46777	0.01	3.9074	No	3
	LP-III	29	0.59470	0.01	3.9074	No	19
Bakreshwar	Gumbel	21	0.97232	0.01	3.9074	No	24
	LP-III	21	0.56432	0.01	3.9074	No	9

Computed by the authors

Table 9. Chi-Squared tests of normality

Monitoring stations	Methods	Chi-Squared						
		Degree of freedom	Statistic	Significance level	Critical value	P value	Reject	Rank
Massanjore	Gumbel	3	5.01050	0.01	11.3450	0.17103	No	31
	LP-III	4	0.22824	0.01	13.2770	0.99396	No	5
Tilpara	Gumbel	3	34.14000	0.01	11.3450	1.85E-07	Yes	42
	LP-III	4	10.22900	0.01	13.2770	0.36740	No	20
Brahmnai	Gumbel	4	3.16660	0.01	13.2770	0.53034	No	20
	LP-III	5	2.58470	0.01	15.0860	0.76370	No	13
Deucha	Gumbel	3	0.69617	0.01	11.3450	0.87410	No	20
	LP-III	2	0.18899	0.01	9.2103	0.90983	No	4
Bakreshwar	Gumbel	2	3.55020	0.01	9.2103	0.16946	No	32
	LP-III	2	1.89550	0.01	9.2103	0.38762	No	24

Computed by the authors

Citation: Bulletin of Geography. Physical Geography Series 2020, 19, http://dx.doi.org/10.2478/bgeo-2020-0009

Hydro-geomorphological drivers of floods

The lower part of the MRB is flood-prone due to its typical relief, geological formations, drainage, climate, soil and vegetation, which are briefly outlined in the following sections.

The elevation map of the study region reveals that there is a progressive diminution of elevation from west to east (Fig. 7a). To understand the flood characteristics and their relationship with elevation, a horizontal intersect from west to east has been drawn that shows that the elevation profile drops abruptly in the upper part of the basin, followed by a mild fall in the middle part. However, in the lower part, the terrain is almost flat, encouraging the water to concentrate to trigger floods (Fig. 7b).

The formation of the MRB bears a long history from Archean to recent times through the Lower Gondwana, Upper Gondwana and Tertiary periods (Dutt and Mukherjee 1977). The Archean formation includes the Granites, Granite-gneisses, biotite-schists, calc-granulites with quartz and peg-

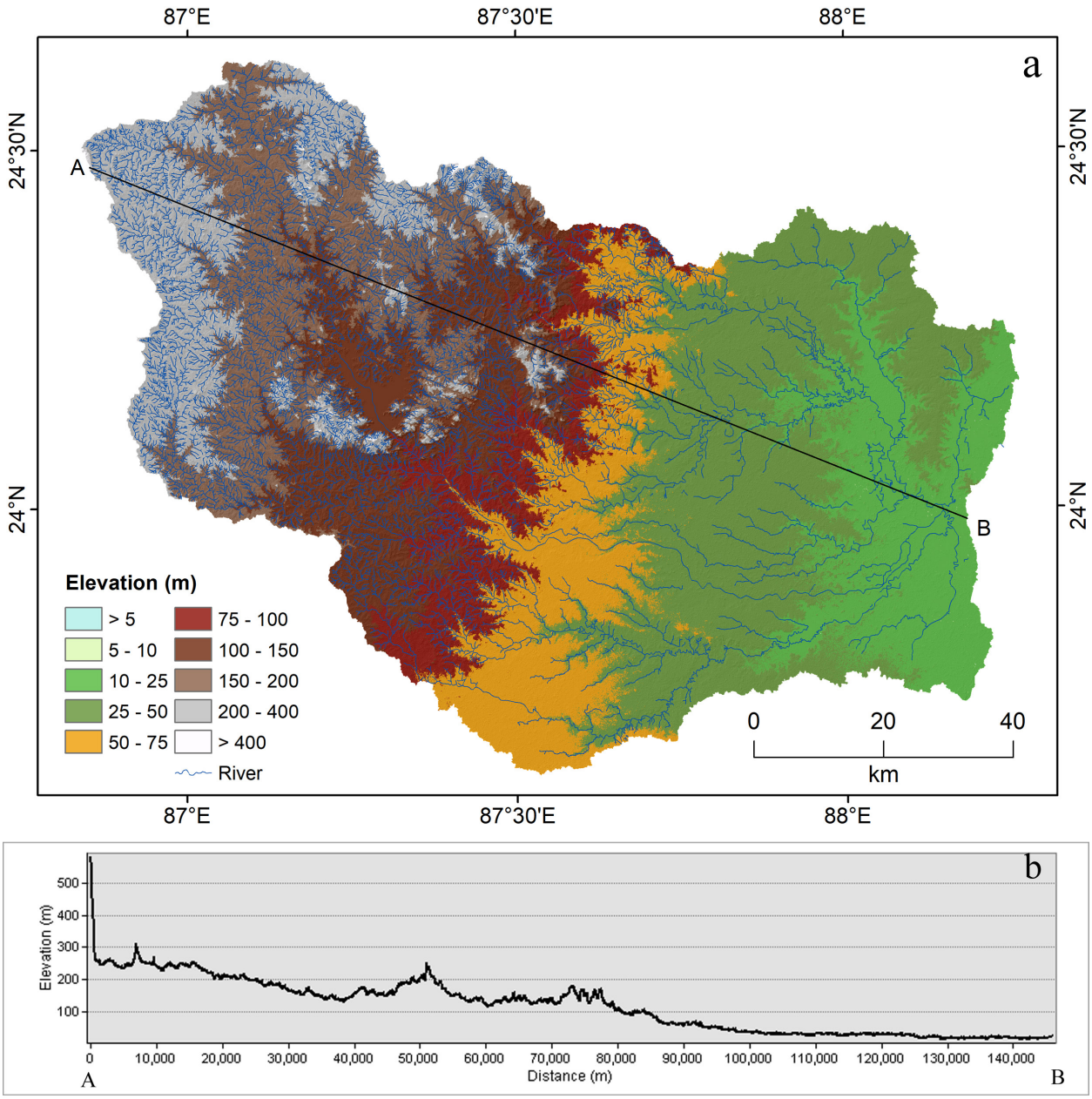

Fig. 7. Elevation of the MRB, a. DEM b. West-East elevation profile (based on SRTM DEM 30 m)

matite veins. The Lower Gondwana formations consist of Talcher formations (Greenish shales, greenish sandstones and boulder beds) and Barakar formations (Gritty sandstones, carbonaceous shales, sandy slates, coal seams and conglomerates). Similarly, Upper Gondwana formations consist of the Dubrajpur stage (Ferruginous sandstones, grits, shales and clays) and the Rajmahal stage (Basalt) separated by the Inter-trappen beds. Besides, the Tertiary formation consists of Ferruginous and felspathic sandstones. The recent formation includes laterites and lateritic gravel with fossil wood and alluvium. Most of the upper parts of the basin are composed of Granites and Granite-Gneiss (Fig. 8a). The

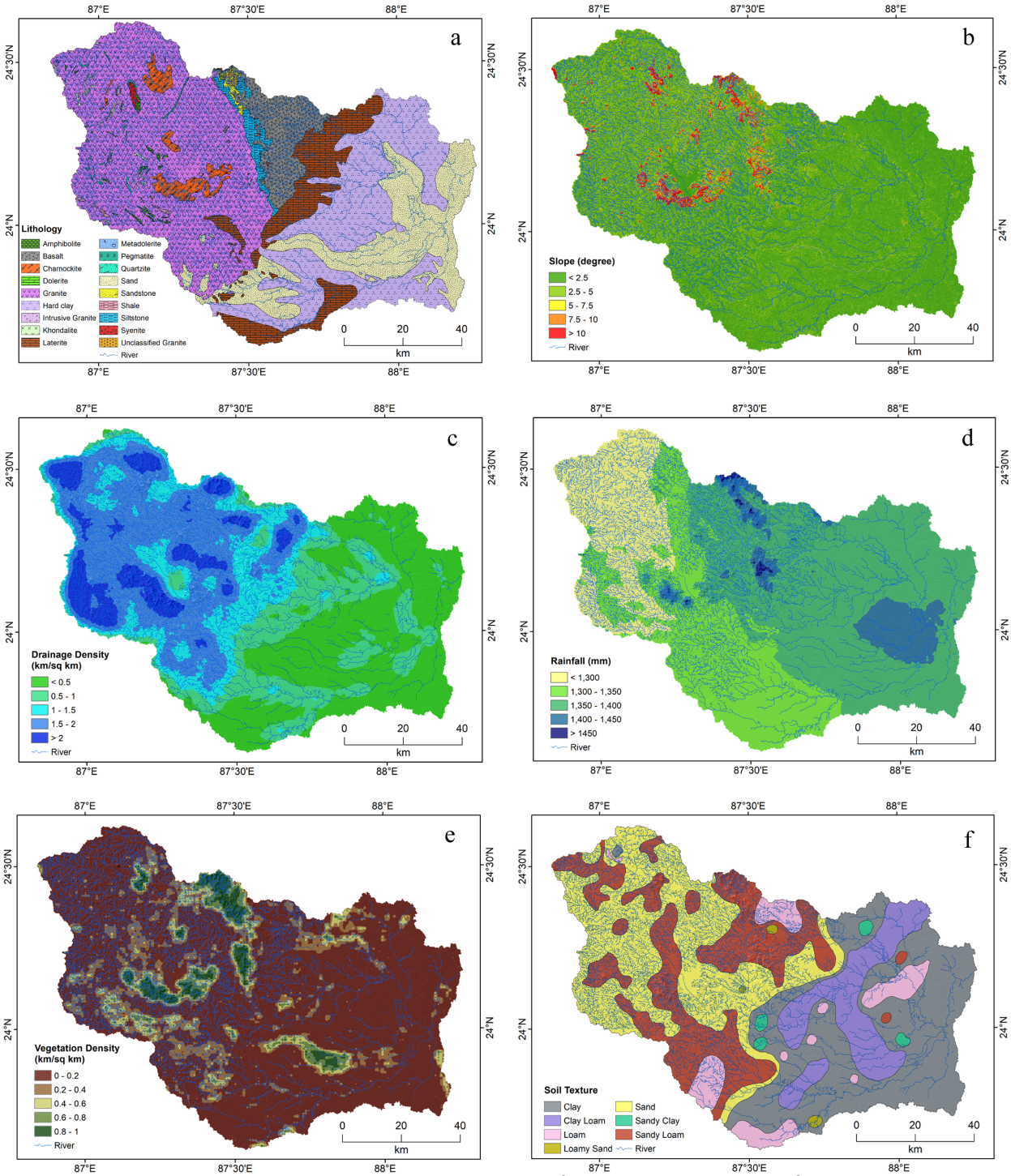

Fig. 8. Basin Characteristics a. Geology (Source: District Resource Map of Birbhum and Murshidabad of West Bengal and Devghar, Dumka, Sahibganj of Jharkhand, GSI), b. Average slope of the Mayurakshi River Basin (Computed from SRTM DEM 30m), c. Drainage density of the Mayurakshi River Basin (Computed from SoI topographical maps, 1:50000), d. Rainfall of the Mayurakshi River Basin (Source: WorldClimb- Global Climate Data), e. Vegetation of the Mayurakshi River Basin (Source: Landsat-8 OLI, 15/01/2017), f. Soils of the Mayurakshi River basin (Source: Chakrabarti 1985)

Citation: Bulletin of Geography. Physical Geography Series 2020, 19, http://dx.doi.org/10.2478/bgeo-2020-0009

middle part of the river basin is mostly characterised by the deposition of Laterites, Basalt, and hard clays impregnated with Caliche nodules. The lower catchment is mostly characterised by recent alluvial deposition of alternate layers of sand, silt and clay attributed by alluviation of river diversion, flooding and consequent shaping by the twin action of the Kuea (a right-bank tributary of the Mayurakshi) and the Dwarka (a left-bank tributary of the Mayurakshi). Thus, the upper part, having impervious structure, encourages rapid surface run-off under the higher magnitude of slope, which triggers flood in the lower stretch.

The average slope of the Mayurakshi River Basin reveals that the slope ranges from about 0˚ (zero) to 44.24˚ and is categorised into five classes: low (<2.5˚), moderately low (2.5˚–5˚), moderate (5˚–7.5˚), moderately high (7.5˚–10˚) and high (>10˚) (Fig. 8b). The eastern part of the entire river basin falls into the low average slope, which is a low floodplain formed by the combined depositional action of the Mayurakshi and the Bhagirathi River. The areas of gentle slope cover the part of plateau fringe and a few areas of plateau proper that are intensively dissected by numerous gullies. The moderate and moderately high slope is found in the limited parts of the erosional plateau. The high average slope is found in the source region of the river and the residual hill areas scattered in the upper part of the basin. This basic slope composition drives flood in the lower stretch of the river system.

The Mayurakshi River Basin is drained by the Mayurakshi and its three tributaries, namely the Dwarka, the Kuea and the Brahmani. All these rivers contain many tributaries while passing through their course. The drainage density of the entire river basin varies from 0 (zero) to 2.88 which has been divided into five categories: low (0–0.5), moderately low (0.5–1), moderate (1–1.5), moderately high (1.5–2), high (>2) (Fig. 8c). Low to moderately low drainage density is found in the entire eastern part of the river basin, which is the lower part of the river characterised by the depositional plain of older alluvium lacking conspicuous relief. Moderately high drainage density is observed in the middle part of the entire river characterised by low relief, gentle slope and colluvium soil with high porosity. Moderately high drainage density is located in the catchment area of the river basin. This area is basically partly plateau fringe and partly plateau proper and is characterised by undulating topography with a perceptible slope where a number of tributaries are found to be initiated and join to the major river. The highest drainage density is found in the few areas of the river basin that are located basically in the source region of the Brahmani, the Dwarka, the Kuea and the Mayurakshi. These areas are hilly tract composed of shale, sandstone and basaltic rock where most of the rivers run on a basaltic rock with such high energy that they completely erode the basaltic rock and finally pave their way on shale and sandstone. This typical drainage characteristic with its underlying substratum induces rapid movement of the water from the upper part of the MRB and the concentration of floodwater in its lower stretch.

The Mayurakshi River Basin falls basically in a hot and humid monsoon type of climate. The climate of this river basin is largely determined by the proximity of the Bay of Bengal to the south, Chhotonagpur plateau in the north-east, and the Himalaya to the north. The variability of rainfall has been observed over the entire basin. The south-west monsoon appears in May and prevails up to the second week of October, having a high rain-bearing cloud to trigger high-intensity rainfall. The variation of annual rainfall in the river basin ranges from 1,215 to 1,514 mm, which has been classified into five categories: <1,300 mm as low, 1,300–1,350 mm as moderately low, 1,350–1,400 mm as moderate, 1,400–1,450 mm as moderately high and >1,450 mm as high (Fig. 8d). Clear graduation of the intensity of annual rainfall has been observed where the upper, middle and lower parts of the river basin have registered low, moderate and high rainfall, respectively. According to Irrigation and Waterways Directorate, Govt. of West Bengal (2000), it has been observed that average annual rainfall during 2000 was 1,285 mm for the gauge stations of Maharo, Massanjore and Tilpara, and 1,350 mm for the gauge stations Kandi and Narayanpur, while rainfall in the period 18–21.09.2000, was 1,071.6 mm for Maharo, 869 mm for Massanjore, 910.6 mm for Tilpara, 677 mm for Kandi and 747 mm for Narayanpur. This huge rainfall during just four days triggered the colossal flood of 2000 (Mukhopadhyay 2012). Moreover, the recent trend in the rainfall pattern shows a decreasing pattern with increasing variability in the differ-

ent districts located in the MRB (Table 10). This leads to a more fluctuating flood peak with a greater degree of uncertainty to predict.

The principal vegetation cover in the river basin is tropical deciduous. In the river basin, varieties of tropical forests have been observed such as sal-dominated forest, dry mixed deciduous forest in the upper part of the basin and dry grassland, dry deciduous scrub forest and palm-dominated Rarh forest in the lower part of the basin. Most of the land in the basin has very low vegetation density except for a few hills of the river basin (Fig. 8e), which promotes rapid run-off, generating peak floods.

Remarkable textural variation of soils in the entire Mayurakshi River Basin is observed. The upper part of the river basin is a basaltic trap where the dominant soil type is fragile coarse lateritic soil with a sandy and sandy loam textural character (Fig. 8f). These soils are poorly aggregated and water holding capacity is very low. In the middle part of the river basin is the Rarh area characterised by transported lateritic alluvium also known as residual soil. In the lower part, most of the areas are very prone to siltation due to the occurrence of frequent floods. The texture of the soil observed is clay, clay loam and loam, which have high water retention capacity (Chakrabarti 1985). These gradations of the soil texture encourage lower infiltration capacity and higher overland flow to generate floods in the lower MRB.

Anthropogenic drivers of floods

The floods in the MRB are accelerated by multiple anthropogenic interventions such as changing LULC, regulated river regimes and anthropogenic sediment flux. First, alteration of land use and land cover plays an important role in influencing the hydrological regime of the river. The LULC establishes linkages between the upstream and downstream of the river. Any changes in LULC in any part of a river basin give signatures on the fluvial hydrology and sediment flux. The modification of LULC is one of the important causes of the flood and the water budget. The ample alteration of LULC has been noticed in the MRB in 10 years (2005/06 to 2015/16). The lion's share of inland water bodies, including ponds and rivers, decreased from 321.298 km^2 to 281.234 km^2, while settlement area recorded an increase from 831.357 km^2 in 2005/06 to 866.06 km^2 in 2015/16. This typical alteration has induced the flood potential of the MRB (Islam et al. 2020).

The second most influential factor is the regulated river regime. Over the MRB, structural interventions in the form of dams, barrages, weirs and embankments are common that often regulate the hydrological behaviour of the Mayurakshi River system. The massive dams and barrages, especially Massanjore and Tilpara, have resulted in high-frequency low-magnitude events compared to the low-frequency high-magnitude events of the predam phase. The flood frequency started rising continuously as of 1985. The flood frequency doubled (n=15 to 29) during 1990–2010. In brief, though the dams have moderated the flood peak, they have extended the flow duration.

The third is related to the anthropogenic sediment flux. Stone quarrying and stone crushing are the dominant anthropogenic inputs that control both the long profile and cross profile of the river which induces the flood. The stone crushing centre produces a huge quantity of stone chips. A fraction of the stone chips flows from the crushing centre to

Table 10. Trend of rainfall at the selected districts of the MRB

Period	Birbhum (Mean±SD)	Deoghar (Mean±SD)	Dumka (Mean±SD)	Murshidabad (Mean±SD)	Pakaur (Mean±SD)	Sahibganj (Mean±SD)
1901–1950	1423.80 ±172.45	1376.75 ±180.49	1405.87 ±179.08	1441.79 ±152.61	1443.19 ±187.13	1407.50 ±173.44
1951–2002	1338.71 ±269.18	1250.54 ±263.41	1288.30 ±269.32	1378.74 ±248.06	1325.58 ±282.35	1291.05 ±257.18

Computed from rainfall data downloaded from India Water Portal

Citation: Bulletin of Geography. Physical Geography Series 2020, 19, http://dx.doi.org/10.2478/bgeo-2020-0009

the river by overland flow. The deposition of stone chips, in the long run, modifies the bed morphology of a river (Islam et al. 2020). The channel depth and the cross-sectional area have decreased with time, which reduces the cubic capacity of the river, ultimately inducing floods.

Conclusion

The MRB has a long-standing problem of floods that damage settlements, destroy crops and threaten the transport and communication system. Across the five monitoring stations, the highest flood peaks were observed as 8,980 $m^3 s^{-1}$ for Massanjore in 1991 during 1978–2009; 11,330 $m^3 s^{-1}$ in 1978 during 1957–2009 for Tilpara; 2,000 $m^3 s^{-1}$ in the year 2000 during 1981–2009 for Brahmani; 1,270 $m^3 s^{-1}$ in 2000 during 1957–2009 for Deucha; and 710 $m^3 s^{-1}$ for Bakreshwar during 1956–77. Furthermore, the probability density function shows that all the distribution for the five stations is not perfectly normal; rather, a skewed distribution pattern is more common, especially for the Mayurakshi River (Massanjore and Tilpara stations) than the smaller rivers like Brahmani, Dwarka and Kuea. Thus, the hydro-geomorphological characteristics of the MRB and its sub-system are marked by distinct variability of the annual flood discharge. Moreover, future floods have been simulated for 2-, 5-, 10-, 25-, 50-, 100-, and 200-year return periods using both the Gumbel and LP-III, which show that the range of the simulated value is higher for LP-III. The KS, AD and chi-squared test statistics indicate that LP-III is a more reliable and appropriate method for flood simulation compared to Gumbel. Thus, the role of LP-III in understanding the flood dynamics of such a river basin characterised by very fluctuating rainfall and discharge implies its significance in the flood geomorphological study of the monsoon-dominated tropical river basin.

Moreover, the FFA may be effective for framing the policy recommendations to reduce the flood susceptibility of the local people. The MRB is an agro-based river basin where more than 80% of people engaged in agricultural pursuits are worst hit by the variable nature of floods. The simulation in this study may help the planners to better grasp the complexity of the flood behaviour. This may allow them to create an early warning system that may absorb shocks to the agrarian economy and that may confer resilience against this hazard by increasing adaptive capacity and decreasing the exposure to hazard. Moreover, this study may also be effective for the framing of sustainable land-use planning observing the flood depth, frequency and duration of a particular spatial unit. The policy recommendations can be further strengthened if empirical field investigation could be executed for revealing the in-depth socio-economic profile of the study area and livelihood choices of the local people. This opens up a new arena of future research.

Acknowledgements

This paper is the outcome of the Major Research Project sponsored by the Indian Council of Social Science Research (ICSSR), Ministry of Human Resource Development (MHRD) Govt. of India awarded to the first author vide the sanction order no. F.No.02/ 295/201617/ICSSR/RP dated 29.03.2017. We are grateful to the two anonymous reviewers for their constructive comments. Moreover, we acknowledge the kind cooperation received from Mr. Sadik Mahammad, Mr. Suman Deb Barman and Ms. Susmita Ghosh for preparing a few figures.

Disclosure statement

No potential conflict of interest was reported by the authors.

Author contributions

Study design: AI, BS; data collection AI, BS; statistical analysis: AI, BS; result interpretation AI, BS; manuscript preparation AI, BS; literature review: AI, BS.

References

BARNETT V, 1975, Probability plotting methods and order statistics. *Journal of the Royal Statistical Society: Series C (Applied Statistics)* 24(1): 95–108.

BENAMEUR S, 2017, Complete flood frequency analysis in Abiod watershed, Biskra (Algeria). *Natural Hazards* 86: 519–534.

BHAN SK AND TEAM F, 2001, Study of floods in West Bengal during September 2000 using Indian Remote sensing satellite data. *Journal of the Indian Society of Remote Sensing* 29(1–2): 1–2.

BHAT MS, ALAM A, AHMAD B, KOTLIA BS, FAROOQ H, TALOOR AK AND AHMAD S, 2019, Flood frequency analysis of river Jhelum in Kashmir basin. *Quaternary International* 507: 288–294.

BHATTACHARYYA K, 2011, *The Lower Damodar River, India: understanding the human role in changing fluvial environment*. Springer Science and Business Media.

BHATTACHARJEE K AND BEHERA B, 2018, Determinants of household vulnerability and adaptation to floods: Empirical evidence from the Indian State of West Bengal. *International journal of disaster risk reduction* 31: 758–769.

BLACK AR AND FADIPE D, 2009, Use of historic water level records for re-assessing flood frequency: case study of the Spey catchment. *Water and Environment Journal* 23: 23–31. DOI: http://10.1111/j.1747-6593.2007.00105.x

BOBEE BB AND ROBITAILLE R, 1997, The use of the Pearson type 3 and Log-Pearson type 3 distributions revisited. *Water Resources Research* 13(2): 427–443. DOI: http://10.1029/WR013i002p00427

BOBEE B, CAVADIAS G, ASHKAR F, BERNIER J AND RASMUSSEN P, 1993, Towards a systematic approach to comparing distributions used in flood frequency analysis. *Journal of Hydrology* 142(1–4): 121–136.

CHAKRABARTI SC, 1970, Some consideration on the evolution of physiography of Bengal in Chatterjee, Gupta and Mukhopadhyay (Eds) *West Bengal*, Calcutta: l6–29.

CHAKRABARTI B, 1985, A Geomorphological Analysis of the Mayurakshi River Basin. (Unpublished PhD thesis, The University of Burdwan).

CHAUDHURY AK, 1966, On the meteorological conditions responsible for heavy rainfall in Ajay catchment Area. *Indian Journal of Meteorology and Geophysics* 17: 127–132.

CHOW VT, 1964, Statistical and probability analysis of hydrologic data. *Handbook of applied hydrology*, 8–1.

CHOW VT, MAIDMENT DR AND MAYS LW, 1988, *Applied hydrology*. New York: McGraw-Hill.

COHN TA, LANE WL AND BAIER WG, 1997, An algorithm for computing moments-based flood quantile estimates when historical flood information is available. *Water resources research* 33(9): 2089–2096.

CUNNANE C, 2010, Statistical distributions for flood frequency analysis. *Journal of Hydraulic Research*.

DAS B, PAL SC AND MALIK S, 2018, Assessment of flood hazard in a riverine tract between Damodar and Dwarkeswar River, Hugli District, West Bengal, India. *Spatial Information Research* 26(1): 91–101.

DAS B, PAL SC, MALIK S. AND CHAKRABORTTY R, 2019, Living with floods through geospatial approach: a case study of Arambag CD Block of Hugli District, West Bengal, India. *SN Applied Sciences* 1(4): 329.

DASGUPTA A, 2001, *Mayurakshi Jaladhar-Swadhinuttor Bharater ekti anyatama bahumukhi Sech prakalpa* in Sechpatra 7th year, Irrigation and Waterways Department, Government of West Bengal, Kolkata: 5–11.

DOOCY S, DANIELS A, MURRAY S AND KIRSCH TD, 2013, The human impact of floods: a historical review of events 1980–2009 and systematic literature review. *PLoS currents*, 5.

DUTT DK AND MUKHERJEE SK, 1977, Groundwater Development potential of Bihar (unpublished report), Central Ground water Board, Dept. of Agriculture.

GHOSH A, 2003, *Natural resource conservation and environment management*. APH Publishing.

GHOSH M AND GHOSAL S, 2020, Climate change vulnerability of rural households in flood-prone areas of Himalayan foothills, West Bengal, India. *Environment, Development and Sustainability*: 1–26.

GHOSH A AND KAR SK, 2018, Application of analytical hierarchy process (AHP) for flood risk assessment: a case study in Malda district of West Bengal, India. *Natural Hazards* 94(1): 349–368.

GHOSH KG AND MUKHOPADHYAY S, 2015, Hydro-Statistical analysis of flood flows with particular reference to Tilpara barrage of Mayurakshi River, Eastern India. *ARPN Journal of Earth Sciences* 4(2).

GHOSH KG AND PAL S, 2015, Impact of dam and barrage on flood trend of lower catchment of Mayurakshi river basin, eastern India. *European Water* 50: 3–23.

GUHA-SAPIR D, HOYOIS P, WALLEMACQ P AND BELOW R, 2016, Annual disaster statistical review

2016: The numbers and trends. Brussels, Belgium: Centre for Research on the Epidemiology of Disasters.

GUMBEL EJ, 1941, The return period of flood flows. *The Annals of Mathematical Statistics* 12(2): 163–190.

GUMBEL EJ, 1958, *Statistics of Extremes.* New York: Columbia University Press.

GURU N AND JHA R, 2015, Flood frequency analysis of Tel Basin of Mahanadi river system, India using annual maximum and POT flood data. *Aquatic Procedia* 4: 427–434.

HOLMES RR, (2014, Floods: Recurrence Intervals and 100-year Floods (USGS). USGS Website Retrieved February 2, 2014, from. http://www.water.usgs.gov/edu/

HOSKING JRM AND WALLIS JR, 2005, *Regional frequency analysis: an approach based on L-moments*. Cambridge University Press.

ISLAM A, LASKAR N AND GHOSH P, 2012, An areal variation of fluvial hazard perceptions of various social groups-A perspective from Rural West Bengal, India. *Indian Streams Research Journal* 2(9): 1–9.

ISLAM A AND BARMAN SD, 2020, Drainage basin morphometry and evaluating its role on floodinducing capacity of tributary basins of Mayurakshi River, India. *SN Applied Sciences* 2: 1087. https://link.springer.com/article/10.1007/s42452-020-2839-4

ISLAM A, BARMAN SD, ISLAM M AND GHOSH S, 2020, Role of Human Interventions in the Evolution of Forms and Processes in the Mayurakshi River Basin. In: *Anthropogeomorphology of Bhagirathi-Hooghly River System in India* (135–187). CRC Press. https://www.taylorfrancis.com/books/e/9781003032373/chapters/10.1201/97810030323735-5

JHA VC AND BAIRAGYA H, 2012, Floodplain planning based on statistical analysis of Tilpara barrage discharge: a case study on Mayurakshi River Basin. *Caminhos De Geografia* 13(43): 326–334.

KAPURIA P AND MODAK S, 2019, An Eco-Hydrological Perspective to Monsoon High Flows in the Ganga-Padma System: Imperatives for Flood Management. *ORF Occasional Paper* 214.

KARMOKAR S AND DE M, 2020, Flash flood risk assessment for drainage basins in the Himalayan foreland of Jalpaiguri and Darjeeling Districts, West Bengal. *Modeling Earth Systems and Environment* 6: 2263–2289.

KAMAL V, MUKHERJEE S, SINGH P, SEN R, VISHWAKARMA CA, SAJADI P AND RENA V, 2016, Flood frequency analysis of Ganga River at Haridwar and Garhmukteshwar. *Applied Water Science:* 1–8.

KAUR H, GUPTA S, PARKASH S, THAPA R AND MANDAL R, 2017, Geospatial modelling of flood susceptibility pattern in a subtropical area of West Bengal, India. *Environmental Earth Sciences* 76(9): 339.

KHAN B AND IQBAL MJ, 2013, Forecasting flood risk in the Indus River system using hydrological parameters and its damage assessment. *Arabian Journal of Geosciences* 6(10): 4069–4078.

KEAST D AND ELLISON J, 2013, Magnitude frequency analysis of small floods using the annual and partial series. *Water* 5(4): 1816–1829.

KUMAR TL, RAO KK, BARBOSA H AND UMA R, 2014, Trends and extreme value analysis of rainfall pattern over homogeneous monsoon regions of India. *Natural hazards* 73(2): 1003–1017.

KUMAR R, 2019, Flood Frequency Analysis of the Rapti River Basin using Log-Pearson Type-III and Gumbel Extreme Value-1 Methods. *Journal of the Geological Society of India* 94(5): 480–484.

KUNDZEWICZ ZW, SU B, WANG Y, XIA J, HUANG J AND JIANG T, 2019, Flood risk and its reduction in China. *Advances in Water Resources* 130: 37–45.

LÁZARO JM, NAVARRO JÁS, GIL AG. AND ROMERO VE, 2016, Flood frequency analysis (FFA) in Spanish catchments. *Journal of Hydrology* 538: 598–608.

MAHMOOD A, 1977, Statistical methods in geographical studies. New Delhi: Rajes Publications.

MCCUEN RH, 1993, *Microcomputer applications in statistical hydrology*. Englewood Cliffs, NJ: Prentice Hall.

MALIK S, PAL SC, CHOWDHURI I, CHAKRABORTTY R, ROY P AND DAS B, 2020, Prediction of highly flood prone areas by GIS based heuristic and statistical model in a monsoon dominated region of Bengal Basin. *Remote Sensing Applications: Society and Environment* 19: 100343.

MAZUMDER SK, 2004, Role of Farakka barrage on the disastrous 1998 flood in Malda (West Bengal). *The Ganges Water Diversion: Environmental Effects and Implications,* Springer, Dordrecht, 39–48.

MOHANTY MP, MUDGIL S AND KARMAKAR S, 2020, Flood management in India: A focussed review on the current status and future challenges. *International Journal of Disaster Risk Reduction*, 101660.

MOLLAH S AND BANDAPADHYAY S, 2014, Population-Development-Environment Interface and Flood

Risk in Murshidabad, West Bengal. In: *Landscape Ecology and Water Management,* Springer, Tokyo, 41–53.

MOLLAH S, 2016, Causes of Flood Hazard in Murshidabad District of West Bengal: Victims' Perceptions. In: *Neo-Thinking on Ganges-Brahmaputra Basin Geomorphology,* Springer, Cham, 99–113.

MUKHOPADHYAY S, 2012, People's perception on the flood and its management in the Mayurakshi Basin. Unpublished Ph. D thesis, Visva Bharati, Santiniketan.

MUKHOPADHYAY S. AND LET S, 2014, Changing Flood Intensity Zone of Dwarka River Basin in Eastern India. Trans. *Inst Indian Geograph* 36(1): 123–132.

MILLINGTON N, DAS S AND SIMONOVIC SP, 2011, The comparison of GEV, log-Pearson type 3 and Gumbel distributions in the Upper Thames River watershed under global climate models. Water Resources Research Report 81, Facility for Intelligent Decision Support, Department of Civil and Environmental Engineering, London.

NICHOLLS R, ZANUTTIGH B, VANDERLINDEN JP, WEISSE R, SILVA R, HANSON S AND KOUNDOURI P, 2015, Developing a holistic approach to assessing and managing coastal flood risk. In: *Coastal Risk Management in a Changing Climate,* Butterworth-Heinemann, 9–53.

Office of the District Magistrate, 2014, Flood preparedness and Management Plan, Murshidabad District. Govt. of West Bengal, Kolkata.

Office of the District Magistrate, 2016, District Disaster Management Plan, Murshidabad District. Govt. of West Bengal, Kolkata.

O'MALLEY LSS, 1914, Bengal District Gazetteers—Murshidabad. The Bengal Secretariat Book Depot, Calcutta.

PEARSON K, 1916, IX. Mathematical contributions to the theory of evolution.—XIX. Second supplement to a memoir on skew variation. *Philosophical Transactions of the Royal Society of London. Series A, Containing Papers of a Mathematical or Physical Character* 216(538–548): 429–457.

PILON PJ AND ADAMOWSKI K, 1993, Asymptotic variance of flood quantile in Log-Pearson type III distribution with historical information. *Journal of Hydrology* 143(3–4): 481–503.

RAHMAN AS, RAHMAN A, ZAMAN MA, HADDAD K, AHSAN A AND IMTEAZ M, 2013, A study on selection of probability distributions for at-site flood frequency analysis in Australia. *Natural Hazards* 69: 1803–1813.

REIS JR DS AND STEDINGER JR, 2005, Bayesian MCMC flood frequency analysis with historical information. *Journal of Hydrology*, 313(1–2): 97–116.

ROY P, PAL SC, CHAKRABORTTY R, CHOWDHURI I, MALIK S AND DAS B, 2020, Threats of climate and land use change on future flood susceptibility. *Journal of Cleaner Production* 272, 122757.

RUDRA K, 2020, Combating Flood and Erosion in the Lower Ganga Plain in India: Some Unexplored Issues. In: *Disaster Studies,* 173–186. Springer, Singapore.

SAGHAFIAN B, GOLIAN S AND GHASEMI A, 2014, Flood frequency analysis based on simulated peak discharges. *Natural Hazards* 71: 403–417.

SAHANA M AND SAJJAD H, 2019, Vulnerability to storm surge flood using remote sensing and GIS techniques: a study on Sundarban Biosphere Reserve, India. *Remote Sensing Applications: Society and Environment* 13: 106–120.

SAHANA M, REHMAN S, SAJJAD H AND HONG H, 2020, Exploring effectiveness of frequency ratio and support vector machine models in storm surge flood susceptibility assessment: A study of Sundarban Biosphere Reserve, India. *Catena* 189: 104450.

SAH S AND PRASAD J, 2015, Flood frequency analysis of River Kosi, Uttarakhand, India using statistical approach. *International Journal of Renewable Energy Technology* 4(8).

SARHADI A, SOLTANI S AND MODARRES R, 2012, Probabilistic flood inundation mapping of ungauged rivers: linking GIS techniques and frequency analysis. *Journal of Hydrology* 458–459: 68–86.

STEDINGER JR AND GRIFFIS VW, 2007, Log-Pearson type 3 distribution and its application in flood frequency analysis. *Journal of Hydrologic Engineering* 482(12).

STEDINGER JR AND COHN TA, 1986, Flood frequency analysis with historical and paleoflood information. *Water Resources Research* 22(5): 785–793.

STEDINGER JR AND GRIFFIS VW, 2008, Flood frequency analysis in the United States: time to update. *Journal of Hydrologic Engineering:* 199–204.

TINGSANCHALI T AND KARIM F, 2010, Flood-hazard assessment and risk-based zoning of a tropical flood plain: case study of the Yom River, Thailand. *Hydrological Sciences Journal–Journal des Sciences Hydrologiques* 55(2): 145–161.

WALTERS RA, 2002, Holocene paleoflood hydrology of the Big Lost River, western Idaho National Engineering and Environmental Laboratory, Idaho. *Geology, Hydrogeology, and Environmental Remediation: Idaho National Engineering and Environmental Laboratory, Eastern Snake River Plain, Idaho*, 353, 91.

WEIBULL W, 1939, The phenomenon of ruptures in solids. Ingenjo¨rsvetenskapsakademiens handlingar 153, 17.

World Commission on Dams, 2000, Dams and development: A new framework for decision-making: The report of the world commission on dams. Earthscan.

YUE S, OUARDA TB, BOBÉE B, LEGENDRE P AND BRUNEAU P, 1999, The Gumbel mixed model for flood frequency analysis. *Journal of Hydrology* 226: 88–100.

ZAR JH, 1999, *Biostatistical analysis*. Delhi: Pearson Education India.

ZHANG Q, GU X, SINGH VP AND XIAO M, 2014, Flood frequency analysis with consideration of hydrological alterations: changing properties, causes and implications. *Journal of Hydrology* 519: 803–813.

Received 10 October 2020
Accepted 7 December 2020